

Normal forms near a saddle-node and applications to finite cyclicity of graphics

F. Dumortier, Y. Ilyashenko and C. Rousseau

CRM-2697

October 2000

Limburgs Universitair Centrum, Universitaire Campus, B-3590, Diepenbeek, Belgique
Department of mathematics, Cornell University, Ithaca, New York 14853, U.S.A.
Département de Mathématiques et de statistique and CRM, Université de Montréal, C.P. 6128, Succursale Centre-Ville, Montréal, Qc, H3C 3J7, Canada.
The second author was supported by part by the grants RFBR 98-01-00455, NSF DMS 997-0372, CDRF RMI-2086. The third author was supported by NSERC and FCAR in Canada.

Abstract

In this note we refine the transformation to smooth normal form for an analytic family of vector fields in the neighborhood of a saddle-node. This refinement is very powerful and allows to prove the finite cyclicity of families of graphics (“ensembles”) occurring inside analytic families of vector fields. It is used in [RZ1] to prove the finite cyclicity of graphics through a nilpotent singular point of elliptic type. Several examples are presented: lips, graphics with two subsequent lips, graphics with a nilpotent point of elliptic type and a saddle-node. We also discuss the bifurcation diagram of limit cycles for a graphic in the lips.

Résumé

Dans cette note nous raffinons la transformation à la forme normale pour une famille analytique de champs de vecteurs au voisinage d’un col-nœud. Ce raffinement est très puissant et permet de montrer la cyclicité finie de familles de graphiques (“ensembles”) apparaissant dans des familles analytiques de champs de vecteurs. Il est utilisé dans [RZ1] pour montrer la cyclicité finie de graphiques passant par un point singulier nilpotent de type elliptique. Plusieurs exemples sont présentés : les “lèvres”, des graphiques avec deux secteurs “lèvres” et un graphique avec un point nilpotent de type elliptique et un col-nœud. On discute aussi le diagramme de bifurcation des cycles limites pour un graphique apparaissant dans les “lèvres”.

1. INTRODUCTION

In the study of planar vector fields the question of finite cyclicity of graphics is an important one. Two currents of research meet there.

On one hand the powerful theorem of Ilyashenko-Yakovenko [IY] proves that elementary polycycles have finite cyclicity inside generic families of smooth vector fields. The genericity conditions appearing in the theorem are implicit. Special theorems by many authors give specific genericity conditions on particular graphics (and not on families of vector fields) yielding finite cyclicity inside smooth families of vector fields. The graphics may be elementary or not. However it can be very difficult in practice to check the genericity conditions for a particular graphic.

On the other hand it is conjectured [R1] that graphics occurring among analytic families depending on a finite number of parameters have finite cyclicity inside the given family. A variant of this idea is the basis of the program [DRR] to prove that there exists a uniform bound for the number of limit cycles of a quadratic system. Particular theorems exist proving the finite cyclicity of special graphics (for instance homoclinic loops) inside analytic families depending on a finite number of parameters.

The present note is a contribution to both directions in the particular context of analytic vector fields. We focus our attention to graphics which occur in “ensembles”. The idea is to consider the full “ensemble” (family of graphics), including the bordering graphic(s) which may or may not have higher codimension. We exploit additional data available or easily computable in the neighborhood of the bordering graphic(s) and “push” the information by analytic extension to all graphics of the “ensemble”.

As far as the second direction is concerned the method presented here is very powerful. In particular it has allowed substantial progress in the proof of the finiteness part of Hilbert’s 16th problem for quadratic vector fields, namely the existence of a uniform bound for the number of limit cycles for quadratic systems. The problem has been reduced to the proof that 121 graphics have finite cyclicity inside quadratic systems [DRR]. In that spirit the results of Section 2 have allowed to prove in [DGR] the finite cyclicity of graphics (I_{14a}^2) and (I_{15a}^2) among quadratic systems (names from [DRR]). In this paper we apply our theorem of finite cyclicity of a graphic through a nilpotent elliptic point and a saddle-node (Figure 1) to the graphic (I_{10a}^2) inside quadratic systems (Figure 2).

The results of section 2 are also used in [RZ1] to prove the finite cyclicity of an hp-graphic (i.e starting from a hyperbolic sector and ending in a parabolic sector) through a nilpotent elliptic point. They will be essential to prove the finite cyclicity of 12 more graphics: (F_{6b}^1) , (I_{17b}^2) , (I_{5b}^1) , (I_{18b}^2) , (H_{10}^3) , (I_{7b}^1) , (I_{8b}^1) , (I_{26}^2) , (I_{10b}^1) , (I_{39}^2) , (I_{11a}^1) and (I_{40}^2) , mostly treated in [RZ2]. In all cases the basic idea is that, when considering ensembles, it may happen that, although a genericity condition on a regular transition map cannot be calculated in general, it can be calculated on a particular graphic of the family. Then, using analyticity, it is possible to push the genericity condition to all graphics of the ensemble.

In [IY1] integrable C^k normal forms for unfoldings of saddle-nodes were found. These normal forms allow the explicit calculation of Dulac maps in the neighborhood of the singular point. In this paper we improve this theorem for analytic vector fields: it is possible to choose the normalizing coordinates to be analytic for the critical parameter value everywhere near the saddle-node except for the stable (unstable) one-dimensional invariant manifold passing through the saddle-node itself.

The genericity condition that implies finite cyclicity is formulated as the nonlinearity of some maps along the orbits, written in the normalizing charts. The main trick used in the paper is that the nonlinearity of an analytic map may be established far away from the domain where it is used and then “pushed forward” by analytic extension.

In this way we establish finite cyclicity of graphics that occur in ensembles. The main ensemble under consideration is called “lips”; it is formed by two saddle nodes of opposite attractivity with a connection between two hyperbolic sectors and a continuous family of connections between two parabolic sectors, see Figure 3a. The name was given in [KS], where the ensemble is met under the number (3.13) of the “Kotova zoo” of graphics appearing in typical 3-parameter families of planar vector fields. Without increasing the degeneracy of the vector field one can meet special graphics on the boundary of the ensemble. Denote the orbit (part of the graphic) that connects two saddle-nodes through their hyperbolic (resp. parabolic) sectors as hh- (resp. pp-) connection. If an orbit emerges from one saddle-node through its parabolic sector and enters another one along the boundary between its hyperbolic and parabolic sector it is labeled as a bp-connection. Lips with a pp-connection through a saddle and lips with a bp-connection are shown

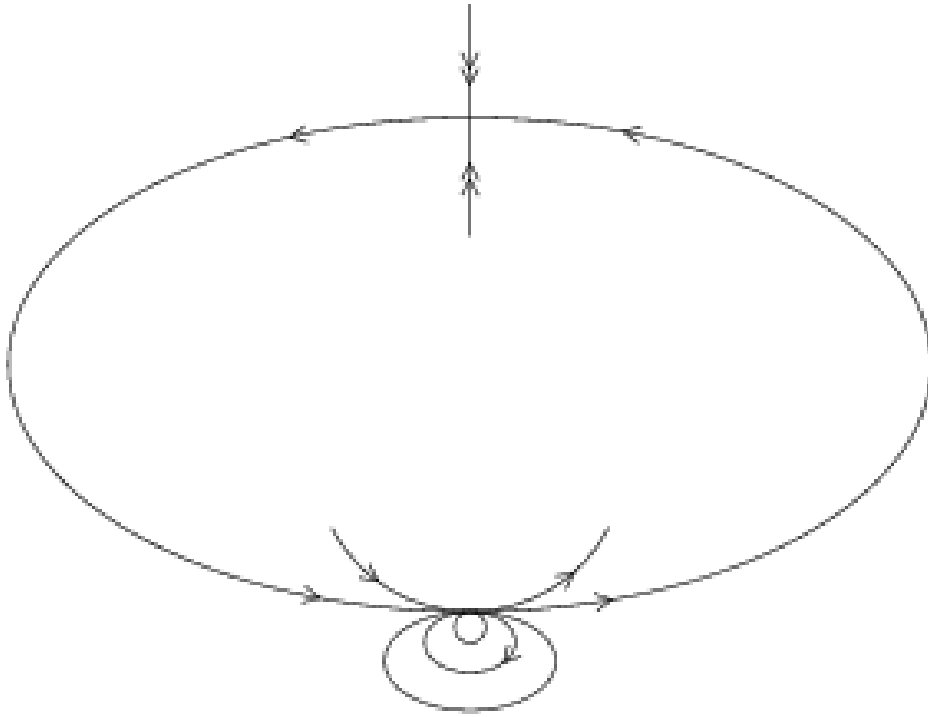


FIGURE 1. Graphic with pp -passage through a nilpotent elliptic point and a saddle-node

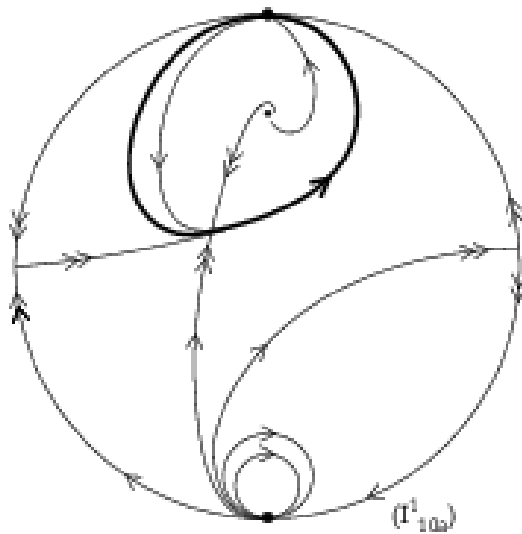


FIGURE 2. Graphic (I_{10a}^1) inside quadratic systems

in Figure 3b, c.

We prove the finite cyclicity of *any* graphic of the ensemble “lips” in an analytic family under one of the following conditions:

- the ensemble has a pp -connection through a saddle (Figure 3b) with either the hyperbolicity ratio r not equal to 1 or with $r = 1$, but with no analytic first integral near the saddle;
- the ensemble has a bp -connection (no extra assumption on the corresponding boundary graphic is required.) As a corollary we obtain the finite cyclicity of any graphic in the ensembles “spadesuit” and “malignant frown”, names from [KS], see Figure 4.

Moreover, we prove the finite cyclicity of any graphic in the ensemble combined by two lips with two hh-

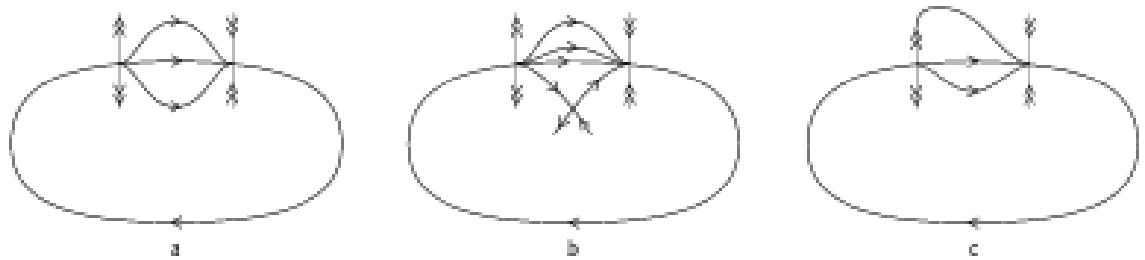


FIGURE 3. Ensembles of graphics of “lips” type

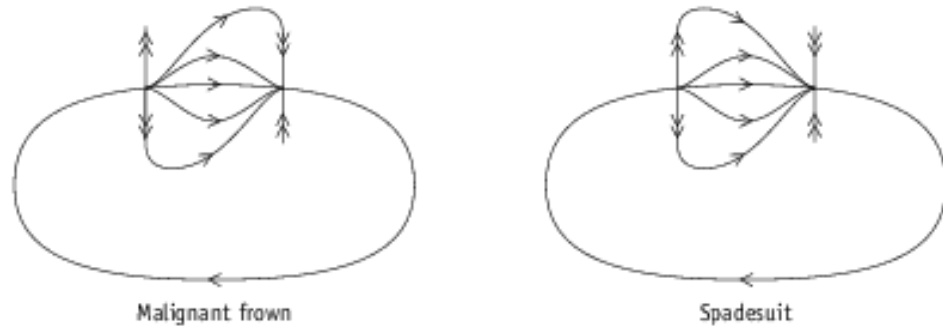


FIGURE 4

connections, (see Figure 5) under a genericity condition. In analytic vector fields the genericity condition can as before be proved locally and pushed far away by analytic extension.

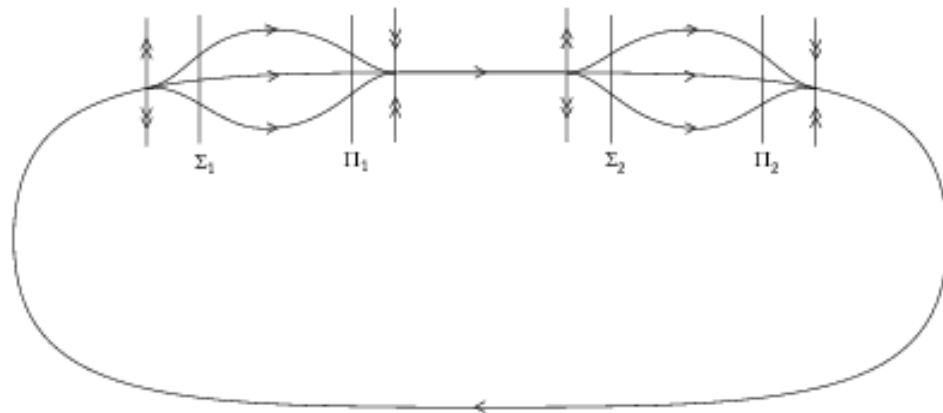


FIGURE 5. Graphics with two lips sectors

Finally in section 5 we discuss the bifurcation diagram for limit cycles appearing by perturbation of a graphic of the lips when the graphic has codimension $n + 1$, i.e. the transition map is nonlinear of order n along the graphic. In that case the graphic has absolute cyclicity n and the bifurcation diagram of the limit cycles contains a trivial 1-parameter family of elementary catastrophes of codimension $n - 1$.

In view of applying our results in specific situations we tackle the problem of calculating the regular pp -transition R . We show, in section 6, the existence of an integral expression of the derivative $\frac{dR}{dy}(y, \lambda)$. The formula is an extension of the traditional formula of Poincaré to express the derivative of a Poincaré mapping along a regular piece of orbit. At the end of section 6 the formula is applied to a specific example.

2. UNFOLDINGS OF ANALYTIC GERMS OF PLANAR SADDLE-NODE VECTOR FIELDS AND ANALYTIC PROPERTIES OF THEIR NORMALIZATIONS.

Unfoldings of germs of planar saddle-node vector fields with singular points of finite multiplicity may be transformed to a polynomial integrable normal form [IY]. The normalizing transformation may be taken

finitely smooth in a neighborhood of a singular point and critical parameter value in the phase-parameter space; the smaller the neighborhood, the smoother will be the transformation. It is impossible, in general, to find an analytic normalizing transformation in some neighborhood, not even a C^∞ one.

Yet some problems of bifurcation theory require analytic properties of the above normalizing transformation. Below we prove the existence of a normalization for the above unfolding which is finitely smooth in the phase-parameter space but which is analytic in the phase space outside the (un)stable manifold at the critical value of the parameter. This result may be applied to the proof of finite cyclicity of some planar polycycles of analytic vector fields as it is shown in the subsequent sections.

2.1. Partially analytic normalization.

A saddle-node is a singular point of a planar vector field at which exactly one eigenvalue is zero. An analytic planar saddle-node germ v of multiplicity $\mu + 1$ is formally orbitally equivalent by means of a transformation $(x, y) \mapsto (z, w)$ to a polynomial normal form

$$v_0 = z^{\mu+1}(1 + az^\mu)^{-1} \frac{\partial}{\partial z} - w \frac{\partial}{\partial w}; \quad (2.1)$$

the time orientation may be reversed. There exists a C^∞ orbital equivalence between v and v_0 [I1]. An unfolding of a germ v , depending on the multi-parameter ε is finitely smoothly orbitally equivalent to the local family

$$v_\varepsilon = P(\varepsilon, z) \frac{\partial}{\partial z} + z^{\mu+1}(1 + a(\varepsilon)z^\mu)^{-1} \frac{\partial}{\partial z} - w \frac{\partial}{\partial w}, \quad (2.2)$$

with $P(\varepsilon, z) = \sum_{i=0}^{\mu-1} b_i(\varepsilon)z^i$ where $b_i(0) = 0$ [IY1].

To state our normalization theorem we need a preliminary normal form of an analytic saddle-node.

Proposition 2.1. *Any complex saddle-node of multiplicity $\mu + 1$ is orbitally analytically equivalent to a germ*

$$v = v_0 + z^{\mu+1}R(z, w) \frac{\partial}{\partial w}. \quad (2.3)$$

This is the germ we will deal with. Main results of this section are the following.

Theorem 1. *Consider a real analytic germ of a saddle-node vector field on $(\mathbb{R}^2, 0)$ with one zero and one negative eigenvalue and with even multiplicity. Then it is C^∞ orbitally equivalent to its normal form (2.1). The equivalence may be taken analytic outside the stable manifold.*

Theorem 2. *Theorem 1 holds for germs with odd multiplicity.*

Theorem 3. *For any C^∞ unfolding of a germ from Theorems 1,2 there exists a finitely smooth orbital equivalence with the polynomial normal form (2.2). For the critical parameter value this equivalence is analytic outside the stable manifold of the saddle-node germ.*

Remark. If the germs of the vector fields in Theorems 1 and 2 (resp. the germ of the family in Theorem 3) depend in an analytic way on extra parameters, not changing the nature of the germ (resp. the family), nor the “formal invariant” $a(0)$ (i.e. $a(\varepsilon) \equiv a(0)$), then the equivalences may be taken analytic in both the variables and the extra parameters in the regions described in the respective theorems.

Theorem 1 is proved below in 2.2 - 2.6. Theorem 2 is a free byproduct of the proof of Theorem 1. Theorem 3 is a simple corollary of Theorems 1 and 2, see 2.7, 2.8.

2.2. Sectorial normalization theorem.

The sectorial normalization theorem (proved in [HKM] and presented in [MR], [I2]) claims that germs v and v_0 are analytically equivalent in some sector-like domains. These domains are described as follows.

Let us divide a small disk $|z| < r$ in 2μ equal sectors with vertex 0; the real axis contains some division rays. Enumerate them counterclockwise beginning with the sector number 1 adjacent from above to the positive real semiaxis. For any sector of this division consider a sector S_j with the same number and bisector, and with opening angle $\alpha \in (\frac{\pi}{\mu}, \frac{2\pi}{\mu})$. The sectors $S_j, j = 1, \dots, 2\mu$ are called *good* ones. They form the covering of the punctured disk $|z| < r$. Let $D = \{|w| < r\}$ be a disk in the w axis, and $\tilde{S}_j = S_j \times D$.

Theorem 2.2 (see [HKM], [MR], [I2]). *Any germ v , see (2.3) in a sector \tilde{S}_j (with r small) is analytically equivalent to v_0 . Moreover, the normalizing map $H_j : \tilde{S}_j \rightarrow \mathbb{C}^2$ has the following properties:*

1. H_j preserves z :

$$H_j(z, w) = (z, h_j(z, w)),$$

and brings v to v_0 ;

2. h_j has asymptotic Taylor series in z with coefficients which are holomorphic functions in w :

$$\hat{h} = \sum_0^{\infty} a_k(w)z^k, \quad a_0(w) \equiv w;$$

\hat{h} is the same for all h_j ;

3. Maps H_j with these properties are unique.

The tuple $H = (H_1, \dots, H_{2\mu})$ is called *the normalizing atlas* of the germ v . Its transition functions generate *the Martinet–Ramis modulus* of the analytic classification of complex saddle-nodes.

Let us call a germ (2.3) *real* if it is real on the real plane.

2.3 Normalizing atlas and Martinet–Ramis modulus.

We do not need to give the complete construction of the above modulus. We only need part of this construction; it is described below.

The (multivalued) function

$$F(z, w) = w f_a(z), \quad f_a(z) = e^{\frac{-1}{\mu z^\mu}} z^a$$

is the first integral of the germ v_0 . Hence, the function

$$F_j = h_j f_a \tag{2.4}$$

is the first integral of the germ v in \tilde{S}_j . In the intersection of their domains, one integral in this list is a holomorphic function of another. We will apply this to two pairs: $F_\mu, F_{\mu+1}$ and $F_1, F_{2\mu}$, thus covering the two real semi-axes in the z -plane. Denote by S^- and S^+ the two sectors:

$$\begin{cases} S^+ = S_1 \cap S_{2\mu} \cap \{\operatorname{Re} z > 0\} \\ S^- = S_\mu \cap S_{\mu+1} \cap \{\operatorname{Re} z < 0\}. \end{cases}$$

Case μ odd. Hence, $f_a \rightarrow 0$ on S^+ as $z \rightarrow 0$, $f_a \rightarrow \infty$ on S^- as $z \rightarrow 0$.

By the previous remark on the first integrals, there exists a holomorphic function ψ^- such that in $S^- \times D$

$$h_{\mu+1} f_a = \psi^-(h_\mu f_a).$$

Let $\psi^-(u) = \psi_0 + \psi_1 u + \psi_2(u)u^2$. Then

$$h_{\mu+1}(z, w) = \psi_0 f_a^{-1}(z) + \psi_1 h_\mu(z, w) + f_a(z) \psi_2(h_\mu f_a) h_\mu^2. \tag{2.5}$$

By statement 2 of Theorem 2.2, $h_{\mu+1} \rightarrow w, h_\mu \rightarrow w$ as $z \rightarrow 0$. But in S^- , $f_a \rightarrow \infty$ as $z \rightarrow 0$. Hence, ψ_0 may be arbitrary, $\psi_1 = 1$ and $\psi_2 \equiv 0$. Summarizing, we get

$$\psi^-(w) = w + C \quad (2.6)$$

$$h_{\mu+1}(z, w) = h_\mu(z, w) + C f_a^{-1}(z). \quad (2.7)$$

The constant C is one component of the Martinet–Ramis modulus.

A parallel consideration gives the relation between h_1 and $h_{2\mu}$, but the result is different because the function f_a on the sector S^+ behaves in an opposite way than on S^- . A second difference comes from the fact that $f_a(z)$ is multi-valued. Hence if we want to compare the value of $f_a(z)$ on $S_{2\mu}$, call it $\bar{f}_a(z)$, with the value of $f_a(z)$ on S_1 we have, on $S_1 \cap S_{2\mu}$, $\bar{f}_a(z) = \nu f_a(z)$ with $\nu = \exp(2\pi i a) \neq 0$. Hence we have:

$$h_{2\mu} \bar{f}_a = \psi^+(h_1 f_a).$$

Let $\psi^+(w) = \psi_0 + \psi_1(w) + \psi_2(w)w^2$. Then an analogue to formula (2.5) holds with $h_{\mu+1}, h_\mu$ replaced by $h_{2\mu}, h_1$. As before, $h_{2\mu} \rightarrow w, h_1 \rightarrow w$ as $z \rightarrow 0$ in S^+ . But now $f_a \rightarrow 0, f_a^{-1} \rightarrow \infty$ as $z \rightarrow 0$ in S^+ . Hence, $\psi_0 = 0, \psi_1 = \nu (= \exp(2\pi i a)), \psi_2$ may be an arbitrary function. Summarizing, we get

$$\begin{aligned} h_{2\mu} &= \bar{f}_a^{-1} \psi^+(h_1 f_a) = \nu^{-1} f_a^{-1} \psi^+(h_1 f_a), \\ \psi^+(0) &= 0, \psi^{+'}(0) = \nu, \end{aligned} \quad (2.8)$$

and ψ^+ is an arbitrary holomorphic function with the above restriction. Roughly speaking, the function ψ^+ is another component of the Martinet–Ramis modulus.

Case μ even. The origin is a topological saddle and we have the same behaviour in S^\pm as the behaviour described above on S^+ .

2.4. Martinet–Ramis modulus in the real case.

Let us call a germ v real if it is real on the real plane.

Proposition 2.3. *If the germ v is real, then*

$$h_\mu(\bar{z}, \bar{w}) = \overline{h_{\mu+1}(z, w)}, \quad h_1(\bar{z}, \bar{w}) = \overline{h_{2\mu}(z, w)}. \quad (2.9)$$

Proof. By assumption, v is invariant under the involution $(z, w) \mapsto (\bar{z}, \bar{w})$ in the source and the target. By the uniqueness of the normalizing atlas, see Theorem 2.2, H has the same property:

$$h_{\mu-k}(\bar{z}, \bar{w}) = \overline{h_{\mu+k+1}(z, w)}, \quad k = 0, \dots, \mu - 1.$$

This proves the proposition. \square

Proposition 2.4. *For the real germ v , the constant C in (2.6) is purely imaginary, and $\text{Im } h_\mu(x, y) = \frac{iC}{2} f_a^{-1}(x)$.*

Proof. Let $(x, y) \in \mathbb{R}^2$. By (2.7) and (2.9)

$$i \text{Im } h_\mu(x, y) = -i \text{Im } h_{\mu+1}(x, y) = -\frac{C}{2} f_a^{-1}(x).$$

Hence, C is purely imaginary. \square

Proposition 2.5. Fix an arbitrary positive $x_0 \in S^+$ and let $g(w) = h_1(x_0, w)$. Let $\beta = g^{-1}(0)$. Then β and $g'(\beta)$ are real.

Proof. Let

$$g_1(w) = h_{2\mu}(x_0, w), \quad c = f_a(x_0).$$

Then, by (2.8)

$$cvg_1 = \psi^+(cg), \quad \psi^+(0) = 0, \psi^{+'}(0) = \nu. \quad (2.10)$$

By (2.9),

$$g(\bar{w}) = \overline{g_1(w)}. \quad (2.11)$$

By (2.10) and (2.11), $g(\beta) = 0$ implies $g_1(\beta) = 0 = g_1(\bar{\beta})$. As g_1 is one-to-one, $\beta = \bar{\beta}$, hence β is real.

By (2.10)

$$cvg'_1(\beta) = \psi^{+'}(0)cg'(\beta),$$

hence, $g'_1(\beta) = g'(\beta)$. By (2.11), and reality of β ,

$$g'(\beta) = \overline{g'_1(\beta)}.$$

Hence, $g'(\beta)$ is real. \square

Remark. The same holds for hyperbolic sectors if μ is odd.

2.5. Automorphisms of the normalized germ.

Proposition 2.6 for parabolic sector. Consider an arbitrary complex number C^- and let

$$H^-(z, w) = (z, h^-(z, w)), \quad h^-(z, w) = w + C^- f_a^{-1}(z). \quad (2.12)$$

Then H^- is an automorphism of the germ v_0 in $\tilde{S}^- = S^- \times D$;

$$(H^-(z, w) - (z, w))|_{\tilde{S}^-} \text{ is flat on } z = 0. \quad (2.13)$$

Proof. The map H^- preserves the z -coordinate and permutes the level curves of the first integral $F = wf_a(z)$ of the germ v_0 . Hence, it preserves the germ itself.

Statement (2.13) follows from the analogous property of f_a^{-1} : it tends to zero together with all derivatives when $z \rightarrow 0$ in S^- . \square

Proposition 2.7 for hyperbolic sector. Let φ be an arbitrary holomorphic function with $\varphi(0) = 0, \varphi'(0) = 1$. Let

$$H^+(z, w) = (z, h^+(z, w)), \quad h^+(z, w) = f_a^{-1}(z)\varphi(wf_a(z)). \quad (2.14)$$

Then H^+ is an automorphism of the germ v_0 in $\tilde{S}^+ = S^+ \times D$;

$$(H^+(z, w) - (z, w))|_{\tilde{S}^+} \text{ is flat on } z = 0. \quad (2.15)$$

Proof. H^+ preserves v_0 for the same reason as H^- .

Statement (2.15) follows from the analogous property of f_a in S^+ . Namely, let $\varphi(w) = w + \varphi_2(w)w^2$. Then

$$h^+(z, w) = w + f_a(z)\varphi_2(wf_a(z))w^2.$$

This implies (2.15). \square

2.6. Smooth normalization of a saddle-node germ analytic outside the stable manifold for even multiplicities.

Here we prove Theorem 1. A real saddle-node (2.3) with even multiplicity has three sectors: one parabolic and two hyperbolic. The stable invariant manifold separates them. In the preliminary normal form (2.3) it is $x = 0$. We will call the union of two hyperbolic sectors in $x > 0$ *the hyperbolic part* (of the neighborhood of the saddle-node).

The normalizing map H will be constructed separately in the open parabolic sector ($x < 0$) and in the hyperbolic part. Both maps will be analytic in their domains and have flat difference with the identity on $x = 0$. Hence, after extension by the identity at $x = 0$, one becomes a C^∞ continuation of the other.

In the parabolic sector let $H = H^- \circ H_\mu$, where H_μ is the same as in Theorem 2.2, H^- is as in (2.12) with the constant C^- well chosen. Namely, let $H_\mu = (z, h_\mu), C$ be the same as in (2.6). Then let $C^- = \frac{C}{2}$, where C is the component of the Martinet–Ramis modulus, the same as in Proposition 2.4. Then H^- is an automorphism of v_0 in $S^- \times D$ by Proposition 2.6. Hence, H conjugates v and v_0 in the parabolic sector and is real there. Namely, by Proposition 2.4,

$$H(x, y) = (x, \operatorname{Re} h_\mu(x, y))$$

in the parabolic sector.

Let us now construct the map H in the hyperbolic part. It will be taken in the form $H = H^+ \circ H_1$, where H_1 comes from the Sectorial Normalization theorem, H^+ is an automorphism provided by Proposition 2.7 for a well chosen φ . Let $H_1(z, w) = (z, h_1(z, w)), x_0 > 0$ be an arbitrary small number and $g(y) = h_1(x_0, y)$.

Let $k(y) = \operatorname{Re} g(y)$ as in Proposition 2.5; k may be holomorphically extended to the complex domain. Let

$$\varphi = k \circ g^{-1}.$$

Then $\varphi(0) = 0$ and $\varphi'(0) = 1$. The map H^+ given by (2.14) is an automorphism of v_0 by Proposition 2.7. Hence, $H = H^+ \circ H_1$ brings v to v_0 . Moreover, H is real on the segment $\sigma : x = x_0$. As H conjugates two real vector fields v and v_0 , it is real in the saturation of σ by the phase curves of v , hence, in the hyperbolic part $x > 0$ of the neighborhood of zero.

Both maps H^+ and H^- differ from the identity by a map flat on $x = 0$. The maps H_μ and H_1 have the same asymptotic expansions on $x = 0$, see statement 2 of Theorem 2.2. Hence, the map H defined above separately in the parabolic sector $x < 0$ and the hyperbolic part $x > 0$ continued by the identity at $x = 0$ is C^∞ smooth. It is real and brings v to v_0 . Theorem 1 is proved.

Proposition 2.8. *When v has an analytic center manifold the constant C in (2.6) takes the value $C = 0$.*

Proof. If the system has an analytic center manifold $w = k(z)$, then modulo a change of variable $w \mapsto w - k(z)$ in (2.3) $R(z, w)$ factors as $R(z, w) = wR_1(z, w)$. This yields in Theorem 2.2 that \hat{h} factors through w , i.e. all $a_j(0) = 0$. The curve $y = 0$ represents a level curve of the first integral (2.4). As obviously the function $y = 0$ is univalued as a function of x there can be no change of determination yielding that $C = 0$ in (2.6). \square

2.7. Saddle-nodes of odd multiplicity.

Here we prove Theorem 2. A real saddle-node with odd multiplicity is topologically equivalent to a saddle. Consider a germ (2.3). It has two hyperbolic parts $x > 0$ and $x < 0$ and a stable manifold $x = 0$. The desired conjugacy on ($x > 0$) is exactly the same as in the proof of Theorem 1, see 2.6. The conjugacy in $x < 0$ is now constructed in the same way as in $x > 0$. As before let the conjugacy be the identity on $x = 0$. The transformation thus constructed is C^∞ for the same reason as in 2.6. Theorem 2 is proved.

2.8. Partially analytic normalization of unfoldings of saddle-nodes.

Here we prove Theorem 3.

Step 1. Let ε be the (multidimensional) parameter of the unfolding. Let us normalize the saddle-node for $\varepsilon = 0$ according to Theorems 1,2, and extend the normalizing transformation cylindrically in ε . We will get a family of vector fields normalized on the plane $\varepsilon = 0$. The normalizing transformation on $\varepsilon = 0$ has the required properties.

Step 2. Now we can transform the new family to the form

$$v_\varepsilon = w(x, \varepsilon) \frac{\partial}{\partial x} - T(x, \varepsilon) y \frac{\partial}{\partial y},$$

v_0 has the normal form (2.1) (in particular, $T(x, 0) \equiv 1$), by a finitely smooth map, *identical on $\varepsilon = 0$* [B]. Division by T brings v_ε to

$$\tilde{v}_\varepsilon = w_1(x, \varepsilon) \frac{\partial}{\partial x} - y \frac{\partial}{\partial y}, \quad w_1(x, 0) = x^{\mu+1} (1 - ax^\mu)^{-1}.$$

Step 3. The normalization procedure from [IY1], see also [IL], §9.2, allows us to normalize the family $w_1(x, \varepsilon) \frac{\partial}{\partial x}$ preserving $w_1(x, 0)$ by a finitely smooth map which is identical on $\varepsilon = 0$. The cylindrical extension in y of the latter map brings \tilde{v}_ε to the normal form (2.2).

The composition of maps constructed in Steps 1-3 provides the desired transformation.

3. FINITE CYCLICITY OF GRAPHICS OCCURING IN THE LIPS

To prove the finite cyclicity of the different graphics discussed in this section we bring the family of vector fields to C^k normal form in the neighborhood of the singular points. We introduce sections transversal to the graphics in the neighborhood of the singular points. We use the freedom of choice in the normalizing coordinates to simplify the regular transitions defined on the sections. We introduce generic conditions on the regular transitions which are always defined (domain and image) in the normalizing coordinates. These generic conditions are always intrinsic (independent of the normalizing coordinates).

We repeat briefly the finite cyclicity proof for a particular graphic of the lips as it will be used later in Section 3 and in Sections 5 and 6.

3.1 Finite cyclicity of polycycles inside lips.

Theorem 3.1 [EM]. *Consider a C^∞ planar vector field v_0 with an ensemble of graphics of the type “lips”: two saddle-nodes of opposite attractivity with one hh-connection, and a continuum of pp-connections. Suppose that the regular pp-transition, written in normalizing coordinates near the saddle-nodes has a nonzero derivative of order $n \geq 2$ at some point a (Figure 6). Then the graphic of the ensemble passing through a has finite cyclicity not greater than n .*

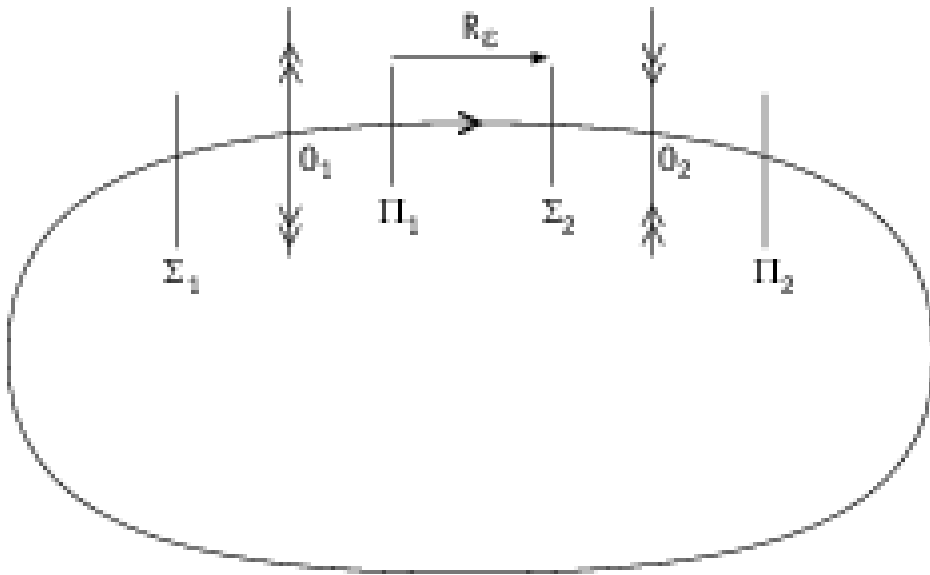


FIGURE 6. Sections for the lips

Proof. Let O_1, O_2 be the saddle-node singular points, the center manifold of O_1 is repelling, that of O_2 is attracting. Consider an arbitrary C^∞ unfolding v_ε of the vector field v_0 . For any k , there exists a neighborhood of any of the saddle-nodes O_1, O_2 in \mathbb{R}^2 and a neighborhood of 0 in the parameter space such that the unfolding has the following normal form:

$$v_\varepsilon^1 = P_1(\varepsilon, x) \frac{\partial}{\partial x} + x^{\mu+1}(1 + a(\varepsilon)x^\mu)^{-1} \frac{\partial}{\partial x} + y \frac{\partial}{\partial y} \text{ near } O_1,$$

$$v_\varepsilon^2 = P_2(\varepsilon, u) \frac{\partial}{\partial u} + u^{\nu+1}(1 + b(\varepsilon)u^\nu)^{-1} \frac{\partial}{\partial u} - v \frac{\partial}{\partial v} \text{ near } O_2.$$

Here P_1 and P_2 are polynomials in x and u respectively, of degree $\mu - 1$ and $\nu - 1$ respectively with ε -depending coefficients vanishing for $\varepsilon = 0$ [IY1]. Let $\Sigma_1, \Pi_1, \Sigma_2, \Pi_2$ be cross-sections near O_1, O_2 given by $x = -\alpha; x = \alpha, |y| \leq \alpha; u = -\alpha; u = \alpha, |v| \leq \alpha, \alpha > 0$ small. Let $x_1 = y|_{\Sigma_1}, y_1 = y|_{\Pi_1}, x_2 = v|_{\Sigma_2}, y_2 = v|_{\Pi_2}$. Then the maps along the orbits of the vector fields v_ε have the following form:

$$\begin{cases} \Delta_1 : \Sigma_1 \rightarrow \Pi_1, & x_1 \mapsto y_1 = \Delta_1(x_1) = M(\varepsilon)x_1 \\ \Delta_2 : \Sigma_2 \rightarrow \Pi_2, & x_2 \mapsto y_2 = \Delta_2(x_2) = m(\varepsilon)x_2, \end{cases}$$

with

$$m(\varepsilon) \rightarrow 0, M^{-1}(\varepsilon) \rightarrow 0$$

as $\varepsilon \rightarrow 0$. The following map is obtained by following the flow

$$R_\varepsilon : \Pi_1 \rightarrow \Sigma_2, y_1 \mapsto x_2 = R_\varepsilon(y_1),$$

Moreover, the normalizing charts $(x, y), (u, v)$ may be chosen so that the hh -transition is a mere translation ([GR]):

$$\Delta_3 : \Pi_2 \rightarrow \Sigma_1, y_2 \mapsto x_1 = y_2 + \delta(\varepsilon).$$

Remark. Let Π_1 be parametrized by y_1 and a be the y_1 -coordinate of the intersection of the graphic with Π_1 , as in Theorem 3.1. The assumption of the theorem is:

$$R_\varepsilon^{(n)}(a) \neq 0,$$

for some $n \geq 2$.

It is invariant with respect to the choice of normalizing coordinates [GR]. Indeed, the transition map from one normalizing chart (x, y) to another $(x, z(x, y))$ is merely a shift on $\Pi_1 : z(\alpha, y) = y + \delta$. The same holds for Σ_2 .

End of the proof. Consider two maps of Π_1 to Σ_2 , corresponding to forward and backward moving along the orbits of v_ε :

$$R_\varepsilon : \Pi_1 \rightarrow \Sigma_2, y_1 \mapsto R_\varepsilon(y_1),$$

$$\Delta_2^{-1} \circ \Delta_3^{-1} \circ \Delta_1^{-1} : \Pi_1 \rightarrow \Sigma_2, y_1 \mapsto m(\varepsilon)^{-1}M(\varepsilon)^{-1}y_1 - m(\varepsilon)^{-1}\delta(\varepsilon).$$

Zeros of the displacement map

$$V_\varepsilon(y_1) = R_\varepsilon(y_1) - m(\varepsilon)^{-1}M(\varepsilon)^{-1}y_1 + m(\varepsilon)^{-1}\delta(\varepsilon)$$

correspond to periodic orbits. Although V_0 does not exist $V_\varepsilon^{(n)}|_{\varepsilon=0}$ does exist and we have $V_\varepsilon^{(n)}|_{\varepsilon=0}(a) = R_0^{(n)}(a) \neq 0$. Hence, $V_\varepsilon^{(n)}(a) \neq 0$ for small ε . By Rolle's theorem, V_ε has no more than n zeros near a . This proves the theorem. \square

3.2 Lips with typical boundary graphics inside analytic families.

Theorem 3.2.

- (1) *If the ensemble formed by lips has a pp-boundary graphic passing through a hyperbolic saddle inside an analytic vector field then any graphic of the ensemble has absolute finite cyclicity as soon as the saddle has hyperbolicity ratio r different from one or has no analytic first integral. (The hyperbolicity ratio is the absolute value of the quotient of the negative eigenvalue to the positive one).*
- (2) *If the ensemble formed by lips has a bp-boundary graphic inside an analytic vector field then any graphic of the ensemble has absolute finite cyclicity. In particular all graphics inside the malignant frown or the spadesuit have finite cyclicity.*

Proof. We need to prove in each case that the regular pp -transition written in normalizing coordinates has a nonaffine ∞ -jet at each point. This property is invariant under the choice of the normalizing coordinates. By Theorems 1 and 3 these coordinates may be chosen to be analytic on the cross-sections Π_1 and Σ_2 . Hence, in these coordinates, R_0 is analytic. To check that all its ∞ -jets are nonaffine it is sufficient to prove that the map is nonaffine globally.

- (1) To do that in case (1), let us consider the map R_0 near the intersection of Π_1 with the boundary graphic Γ . Making a shift, we can consider the points $\Gamma \cap \Pi_1$ and $\Gamma \cap \Sigma_2$ to have zero y_1 and x_2 coordinates. Then, near 0,

$$R_0(y_1) = \begin{cases} y_1^r(A + O(y_1)), & r \neq 1, \\ y_1(A + \sum_{j=1}^{i-1} c_j y_1^j + B y_1^i \ln y_1 + O(y_1^i)) \text{ for some } i \geq 1; & r = 1, \end{cases}$$

with $AB \neq 0$. This map is not affine near zero. Hence, it is nonaffine everywhere, by analyticity.

- (2) In the case of a bp -boundary graphic the unstable manifold γ of one saddle-node, say O_1 , enters the other saddle-node O_2 as part of a center manifold. Without loss of generality, after a coordinate shift, if necessary, we may assume that $R_0(0) = 0$. Let $\Sigma_2 \cap \gamma = a$, $D = [0, a]$. Then all the positive semi-orbits that begin near O_1 in the domain being a square $K : x_1 \in [0, \alpha]$, $y_1 \in [0, \alpha]$, α is small, in the normalizing chart, intersect D . The map $K \rightarrow D$ along the orbits is analytic. Suppose that $\Pi_1 \supset \{x_1 = \alpha, y_1 \in [0, \alpha]\}$, and the map $R_0 : \Pi_1 \rightarrow D$ is affine. As $R_0(0) = 0$ it is linear; let $R_0(y_1) = \beta y_1$. For any $n > 2$, let $\bar{\Pi}_n = \{x_1 = \frac{\alpha}{n}, y_1 \in [0, \alpha]\}$. The map $R_n : \bar{\Pi}_n \rightarrow D$ along the orbits of the ensemble is well defined and analytic. The map $\bar{\Pi}_n \rightarrow \Pi_1$ may be easily calculated, because $y_1 e^{\frac{1}{\mu x_1^{\mu}} x_1^{-a}}$ is a first integral near O_1 . This map is a multiplication by

$$C_n = e^{\frac{n^{\mu}-1}{\mu \alpha^{\mu}} n^a}, C_n \rightarrow \infty$$

as $n \rightarrow \infty$. Then the map $\bar{\Pi}_n \rightarrow D$ along the orbits is a multiplication by $C_n \beta$. The length of the image is $C_n \alpha \beta$. It tends to infinity with n , but the image belongs to the segment D , a contradiction.

□

3.3 Two subsequent lips.

Theorem 3.3. *A C^∞ vector field with four saddle-nodes of even multiplicity, alternately attracting and repelling, has finite cyclicity if the two regular pp -transitions satisfy the following generic conditions:*

- i) *both are nonaffine at some finite order;*
- ii) *at some finite jet level one map is not right-left affine equivalent through orientation preserving affine maps to the inverse of the other.*

An explicit bound for the cyclicity is given by the minimal order N of the jet of the two pp -transitions on which we can check the genericity condition.

If the two regular pp -transitions are analytic, then the theorem follows under the hypothesis that the transitions are not affine and one map is not right-left affine equivalent through orientation preserving affine maps to the inverse of the other. Indeed these conditions can be verified on a finite jet.

Proof. Denote the cross-sections in the parabolic sectors of the saddle-nodes as $\Sigma_1, \Pi_1, \Sigma_2, \Pi_2$, see Figure 5.

Let $f_\varepsilon : \Sigma_1 \rightarrow \Pi_1$, $g_\varepsilon : \Pi_2 \rightarrow \Sigma_2$ be the pp -transitions corresponding to the value ε of the parameter (g_ε is the transition backwards). For those values of the parameter for which all the saddle-nodes vanish, the maps along the orbits of perturbed fields $a : \Pi_2 \rightarrow \Sigma_1$, $b : \Sigma_2 \rightarrow \Pi_1$ are affine in the normalizing coordinates chosen above.

The displacement map has the form $V_\varepsilon : \Pi_2 \rightarrow \mathbb{R}$, $V_\varepsilon(x) = f_\varepsilon \circ a - b \circ g_\varepsilon$.

Let $f = f_0$, $g = g_0$. Theorem 3.3 follows now from the next Lemma. \square

Main Lemma 3.4. *Let functions f, g be C^K diffeomorphisms on a segment, which are, at some finite jet level of order $< K$, nonaffine and not right-left affine equivalent through orientation preserving affine maps. Then for any two points x_0, y_0 there exists $N = N(f, g, x_0, y_0) < K$, U, V small neighborhoods of x_0, y_0 and small C^N neighborhoods of f and g such that the function*

$$\tilde{h}_{a,b} = \tilde{f} \circ a - b \circ \tilde{g}$$

has no more than N zeros in $U \cap a^{-1}V$, where a, b are arbitrary orientation preserving affine maps.

Proof. Let $x_0 = y_0 = 0$, $f^{(m)}(0) = a_m$, $g^{(m)}(0) = b_m$. Let $a = \alpha x + \alpha_0$, $b = \beta x + \beta_0$, $h_{a,b} = f \circ a - b \circ g$. Then $h_{a,b}^{(m)}(0) = \alpha^m a_m - \beta b_m$.

Let $\alpha \geq 1$. Elsewhere we replace $h_{a,b} = 0$ by an equivalent equation

$$b^{-1} \circ f - g \circ a^{-1} = 0$$

and use the symmetry of f and g in the assumptions of the theorem.

Take k such that $a_k \neq 0$. There exist at most a unique (α, β) such that $h'_{a,b}(0) = h_{a,b}^{(k)}(0) = 0$. Hence, as f and g are not right-left affine equivalent, there exists $n \neq k$ such that for all a and b

$$h'_{a,b}(0) = h_{a,b}^{(k)}(0) = 0 \implies h_{a,b}^{(n)}(0) \neq 0. \quad (3.1)$$

Similar values k_1 and n_1 are obtained when we consider the case $\alpha \leq 1$ and we deal with the function $h_{a,b} = b^{-1} \circ f - g \circ a^{-1}$. We will prove that $N(f, g, 0, 0)$ above may be chosen equal to $\max(n, k, n_1, k_1)$.

We will choose U and V so small that for any a and b and for any \tilde{f}, \tilde{g} C^N -close to f, g one of the following three inequalities holds on $V \cap a^{-1}(U)$: $\tilde{h}'_{a,b} \neq 0$, $\tilde{h}_{a,b}^{(k)} \neq 0$, $\tilde{h}_{a,b}^{(n)} \neq 0$.

That one of these inequalities holds depends on the relations between α, β and the derivatives of f and g at 0. Let $a_k > 0$ (we can obtain that by replacing, if necessary, f and g by $-f$ and $-g$ respectively).

Case 1: $b_k < 0$. In this case $\tilde{h}_{a,b}^{(k)} > 0$ on $V \cap a^{-1}U$ for small U and V and \tilde{f}, \tilde{g} C^N -close enough to f, g ; this assumption will not be repeated later on. Indeed,

$$\tilde{h}_{a,b}^{(k)}(x) = \alpha^k c_k - \beta d_k > 0,$$

where c_k is close to $a_k > 0$, d_k is close to $b_k < 0$, $\alpha > 0$, $\beta > 0$.

Case 2: $b_k = 0$. In this case either

$$\tilde{h}'_{a,b} \neq 0 \text{ or } \tilde{h}_{a,b}^{(k)} \neq 0 \text{ on } V \cap a^{-1}(U). \quad (3.2)$$

Let $A_1 = \{(\alpha, \beta) \in \mathbb{R}_+^2 \mid \alpha c_1 - \beta d_1 = 0\}$ where c_1, d_1 range over small neighborhoods of a_1, b_1 . For $(\alpha, \beta) \notin A_1$, the first inequality in (3.2) holds.

For $(\alpha, \beta) \in A_1$, the set $\tilde{h}_{a,b}^{(k)}(x) = 0$ is given by

$$A_k = \{(\alpha, \beta) \in \mathbb{R}_+^2 \mid \alpha^k c_k - \beta d_k = 0\},$$

where c_k ranges in a small neighborhood of $a_k = f^{(k)}(0)$, and $|d_k| < \delta$ (d_k ranges near $b_k = 0$). Then for $(\alpha, \beta) \notin A_k$,

$$\tilde{h}_{a,b}^{(k)} \neq 0 \text{ on } V \cap a^{-1}(U).$$

Moreover,

$$\{\alpha \geq 1\} \cap A_1 \cap A_k = \emptyset$$

for δ small enough. This proves (3.2). Hence, $\tilde{h}_{a,b}$ has no more than k zeros in $V \cap a^{-1}(U)$.

Case 3: $b_k > 0$. In addition to A_1, A_k , consider a set

$$A_n = \{(\alpha, \beta) \in \mathbb{R}_+^2 \mid \alpha^n c_n - \beta d_n = 0\},$$

where c_n, d_n range near a_n, b_n . The choice of n , see (3.1), implies that for $c_1, c_k, c_n, d_1, d_k, d_n$, close enough to $a_1, a_k, a_n, b_1, b_k, b_n$ respectively

$$A_1 \cap A_k \cap A_n = \emptyset.$$

Hence, either (3.2) holds, or $\tilde{h}_{a,b}^{(n)} \neq 0$. This proves the Main Lemma 3.4, hence, Theorem 3.3. \square

The situation of Theorem 3.3 defines an ensemble of graphics with four semi-hyperbolic points indexed by an open subset of \mathbb{R}^2 . We now give conditions so that any graphic of the ensemble occurring inside an analytic vector field has finite cyclicity.

Corollary 3.5. *A graphic of an analytic vector field with four saddle-nodes of even multiplicity alternately attracting and repelling has finite cyclicity if the two ensembles of lips are bounded simultaneous above (resp. below) by two pp-connections (one for each ensemble of lips), each through a hyperbolic saddle and if the two hyperbolic saddles belonging to the two boundary pp-transitions have hyperbolicity ratios r_1 and r_2 satisfying $r_1, r_2 \neq 1$ and $r_1 r_2 \neq 1$ (Figure 7).*

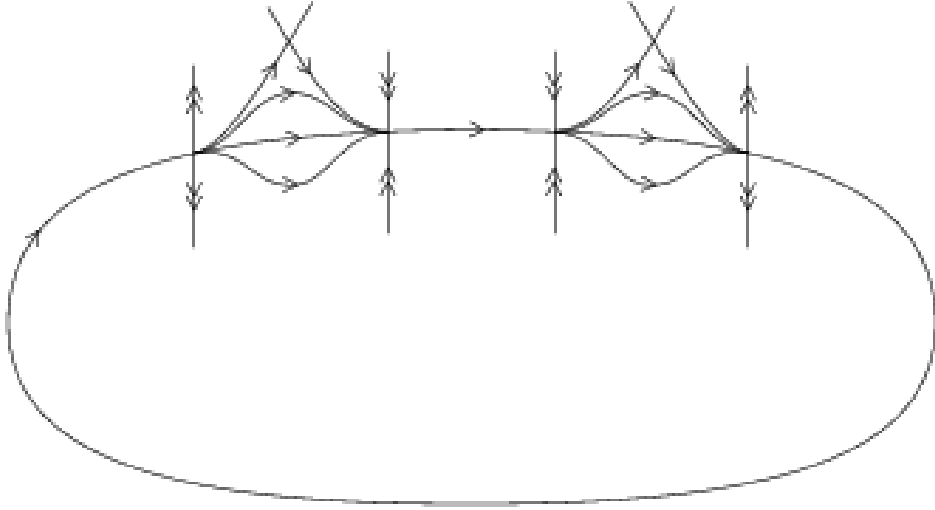


FIGURE 7

Proof. The two pp -transitions are nonaffine: this is the same argument as in Theorem 3.2. We need now to show that one is not right-left affine equivalent to the inverse of the other. For that purpose we use the same sections and notations as in Theorem 3.3 and Main Lemma 3.4.

The sections Σ_i and Π_i can be taken analytic and so as to intersect the pp -boundaries passing through the hyperbolic saddles. Let I and J be the domains of definition of f_0 and g_0 : these domains are open intervals. The intersection points X_0 and Y_0 of the upper pp -boundaries with the sections Σ_i are respectively the supremum of I and J . The maps f_0, g_0 cannot be extended as diffeomorphisms above these points. Indeed, $f_0(X) = (X - X_0)^{r_1}(C + o(1))$, $r_1 \neq 1$, $C > 0$. Hence, $f'_0(X_0) = 0$ for $r_1 > 1$ and $f'_0(X_0) = \infty$ for $r_1 < 1$. The same argument works for g_0 .

Let us suppose that we have a relation of the form

$$f_0 \circ a - b \circ g_0 = 0, \quad (3.3)$$

where a and b are affine maps, the equality standing in the neighborhood of points $y_0 = a^{-1}(x_0)$. The relation can also be written

$$f_0 = b \circ g_0 \circ a^{-1}, \quad g_0 = b^{-1} \circ f_0 \circ a. \quad (3.4)$$

This defines analytic extensions of f_0 on $a(J)$ and of g_0 on $a^{-1}(I)$. Let $a(Y_0) \in I$. Then the first relation in (3.4) leads to a contradiction: f_0 is diffeomorphic at $a(Y_0)$, and $b \circ g_0 \circ a^{-1}$ is not. If $a^{-1}(X_0) \in J$, the second relation in (3.4) provides a contradiction. If none of the case holds, then $a(Y_0) = X_0$. Then (3.3) yields:

$$(Y - Y_0)^{r_1}(C_1 + o(1)) = (X - X_0)^{\frac{1}{r_2}}(C_2 + o(1))$$

which implies $r_1 r_2 = 1$, a contradiction. \square

Corollary 3.6. *A graphic of a C^∞ family of vector fields with an arbitrary number of saddle-nodes, all with central transition, has finite cyclicity as long as there is no more than two pp connections and:*

- (1) *the genericity assumption of Theorem 3.1 is satisfied in the case of one pp-connection;*
- (2) *the genericity assumption of Theorem 3.3 is satisfied in the case of two pp-connections.*

Proof. When there are no pp-connection the saddle-nodes are all of the same attractivity and the graphic is known to have cyclicity one as the derivative of the Poincaré map is far from 1. In the two other cases the proof is exactly the same as the corresponding proof in Theorems 3.1 and 3.3. \square

4. GRAPHIC WITH A SADDLE-NODE AND AN ELLIPTIC NILPOTENT POINT

4.1 Finite cyclicity of such a graphic.

In the next paragraph we are concerned with the finite cyclicity of a graphic through a nilpotent point of multiplicity 3 and of elliptic type inside a C^∞ family of vector fields $v_\varepsilon|_{\{\varepsilon \in \Lambda\}}$. In the neighborhood of such a point the vector field v_0 is C^∞ equivalent to a vector field with 4-jet:

$$\begin{aligned} \dot{x} &= y \\ \dot{y} &= -x^3 + bxy \end{aligned}$$

where $b > 2\sqrt{2}$.

A weighted blow-up $(x, y) = (r\bar{x}, r^2\bar{y})$ allows to study the topological type of the singularity (Figure 8). On the blown-up circle we have two saddles and two nodes.



FIGURE 8. Nilpotent elliptic point and its blow-up

We prefer to transform the singularity via the quasi-homogeneous change of coordinate $(X, Y) = (\frac{x}{c}, \frac{1}{c}(y - cx^2))$ to a system

$$\begin{aligned}\dot{X} &= Y + c^2 X^2 \\ \dot{Y} &= XY,\end{aligned}$$

where $2c^2 - cb + 1 = 0$. Choosing $c = \frac{b - \sqrt{b^2 - 8}}{4}$ (this amounts to choose the bring the two nodes, called P_1 and P_2 , on the blown-up circle to the horizontal axis), letting $c^2 = a$ and renaming (X, Y) by (x, y) we study the singularity with a 4-jet of the form

$$\begin{aligned}\dot{x} &= y + ax^2 \\ \dot{y} &= xy\end{aligned}\tag{4.1}$$

with $a \in (0, \frac{1}{2})$. The same weighted blow-up $(x, y) = (r\bar{x}, r^2\bar{y})$ is used to draw it in Figure 9. The advantage of this model is that the y -axis (corresponding to the direction of approach of the singular point for pp -transitions) is invariant.



FIGURE 9. Nilpotent point of (4.1) and its blow-up

The graphic we will study consists of a connection between the two nodes (for this reason we say that the graphic has a pp -passage through the elliptic point) and an additional saddle-node Q_3 on the connection which we can of course suppose to be attracting (Figure 10).

The genericity condition concerns the passage (regular transition) from P_2 to the saddle-node Q_3 : we consider sections Σ and Π transversal to this transition map. These sections are taken parallel to one coordinate axis in the normalizing coordinates near P_2 and Q_3 .

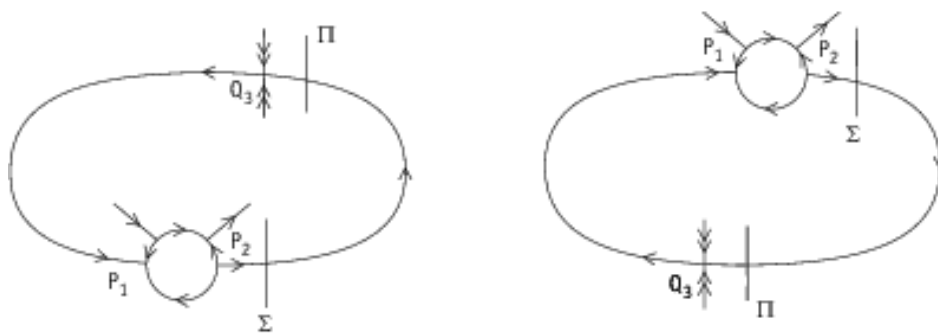


FIGURE 10. Graphic with pp -passage through a nilpotent elliptic point and a saddle-node

(P_2 is considered in the chart $\bar{x} = 1$. Hence the coordinates near P_2 are r and \bar{y} . As $r = 0$ is invariant a normalizing change of coordinates can be taken as a function of the form $\tilde{y} = \bar{y} + O(r) + o(\bar{y})$, which, as P_2 is a node, can be taken analytic if v_0 is analytic.) The regular transition is a map $R : \Sigma \rightarrow \Pi$. Assuming that the connection occurs for $y = 0$ the genericity condition allowing to prove the finite cyclicity is that there exists $n \geq 2$ such that $R^{(n)}(0) \neq 0$.

Remark. The condition is intrinsic. We need to show that the condition is invariant under changes of coordinates preserving the normal form near P_2 and near Q_3 . Near Q_3 the result follows from [GR]. Near P_2 we use that P_2 is a node with normal form (for $\varepsilon = 0$)

$$\begin{aligned}\dot{r} &= r \\ \dot{\tilde{y}} &= \sigma \tilde{y} + Ar^n\end{aligned}$$

where $A = 0$ as soon as $\sigma \notin \mathbb{N}$.

Because of the special form of the system we only allow normalizing changes of coordinates keeping r fixed. If $\sigma \notin \mathbb{N}$ then there is no nonlinear change of normalizing coordinates. Indeed a sufficiently smooth change of coordinate must preserve the analytic invariant manifold. Hence it has the form $\tilde{y} \mapsto \tilde{y}_1 = \tilde{y}(C + O(|(r, \tilde{y})|))$ and must send the first integral $H(r, \tilde{y}) = r^{-\sigma} \tilde{y}$ to $\phi(H)$. From $\sigma \notin \mathbb{N}$ necessarily $\phi(H) = CH$, i.e. $\tilde{y}_1 = C\tilde{y}$. If $\sigma \in \mathbb{N}$ and $A = 0$ we can allow the change of coordinate to have the form $\tilde{y} \mapsto \tilde{y}_1 = C\tilde{y} + o(|(r, \tilde{y})|)$. When $A = 0$, with the same H as before, we get $\phi(H) = CH + D$. On a section $r = r_0$ the first integral H (resp. $\phi(H)$) is an affine map of the normalizing coordinate \tilde{y} (resp. \tilde{y}_1). As ϕ is affine the result follows. We are left with the case $\sigma \in \mathbb{N}$ and $A \neq 0$ in which case the integral has the form $H(r, \tilde{y}) = \frac{\tilde{y} - Ar^\sigma \ln r}{r^\sigma}$. The only allowed change of coordinate preserving the normal form is $\tilde{y} \mapsto \tilde{y}_1 = \tilde{y} + o(|(r, \tilde{y})|)$ and send H to $\phi(H) = H + D$ (which implies that $\tilde{y}_1 = \tilde{y} + Br^\sigma$). We conclude as before since H and $\phi(H)$ are still affine maps of \tilde{y} and \tilde{y}_1 on $r = r_0$.

If n is minimal with this property then we say that the map R is nonaffine of order n at $y = 0$.

Theorem 4.1. *A graphic with central transition through a saddle-node and with pp-passage through a nilpotent elliptic point of multiplicity 3 has finite cyclicity $\leq n$ as soon as the transition map from the elliptic point to the parabolic sector of the saddle-node (in normalizing coordinates, see the previous remark) is nonaffine of some finite order n (Figure 10).*

Proof. We use the method of the blow-up of the family [DRS] and the notations introduced in [RZ1] and we suppose that the saddle-node is attracting. In the neighborhood of the nilpotent elliptic point we can use the following normal form for the family ([RZ1]):

$$\begin{aligned}\dot{x} &= y + a(\varepsilon)x^2 + \mu_2 \\ \dot{y} &= \mu_1 + \mu_3 y + x^4 h_1(x, \varepsilon) + y(x + \eta_2 x^2 + x^3 h_2(x, \varepsilon)) + y^2 Q(x, y, \varepsilon),\end{aligned}\tag{4.2}$$

where $a(0) \in (0, \frac{1}{2})$ and $\eta_2 \in \mathbb{R}$. The parameters are $\varepsilon = (\mu_1, \mu_2, \mu_3, \mu)$, $h_1(x, \varepsilon) = \eta_2 a + O(\varepsilon) + O(x)$. Moreover the functions $h_1(x, \varepsilon)$, $h_2(x, \varepsilon)$ and $Q(x, y, \varepsilon)$ are C^∞ and $Q(x, y, \varepsilon)$ is of arbitrary high order in (x, y, ε) .

We must discuss the number of limit cycles in a Hausdorff neighborhood of the graphic for values of the parameters in a small neighborhood of the origin. Only the parameters μ_i , $i = 1, 2, 3$, will be essential to the results.

We make the change of parameters $(\mu_1, \mu_2, \mu_3) = (\nu^3 \bar{\mu}_1, \nu^2 \bar{\mu}_2, \nu \bar{\mu}_3)$ and consider a neighborhood of the origin in the space (μ_1, μ_2, μ_3) given by $(\bar{\mu}_1, \bar{\mu}_2, \bar{\mu}_3) \in \mathbb{S}^2$ and $\nu \in (0, \nu_0)$.

We will prove that for all $\bar{\mu}^* = (\bar{\mu}_1, \bar{\mu}_2, \bar{\mu}_3) \in \mathbb{S}^2$ and for any μ^* there exist neighborhoods of $\bar{\mu}^*$ and μ^* , there exist $\nu_0 > 0$ and $\delta > 0$ such that for $\bar{\mu}$ and μ respectively in the neighborhoods of $\bar{\mu}^*$ and μ^* and for $\nu < \nu_0$ the family v_ε has at most n limit cycles at a Hausdorff distance less than δ from our graphic. We conclude using compacity of \mathbb{S}^2 .

We identify (4.2) to a $\bar{\mu}$ family of 3-dimensional systems by adding the additional equation $\dot{\nu} = 0$. We take two sections $\Sigma_{1,2} = \{x = \mp x_0\}$ in the neighborhood of the nilpotent point and consider the two transitions $S : \Sigma_2 \rightarrow \Sigma_1$ and $T : \Sigma_1 \rightarrow \Sigma_2$ (Figure 11).

The first transition S is quite standard, except for the fact that Σ_i are two dimensional sections parametrized by (ν, \hat{y}_i) , $i = 1, 2$, where \hat{y}_i are normalized coordinates coinciding for $\nu = 0$ with \tilde{y}_i defined before near P_i (details below). The transition T is not standard as it describes the passage near a non

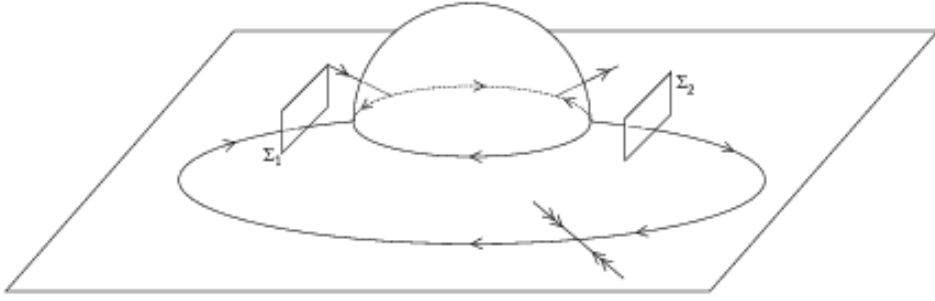


FIGURE 11. The sections Σ_1 and Σ_2 close to the blown-up sphere

elementary singular point. To study it we use the blow-up of the family introduced by Roussarie and applied in [DRS] and [RZ1].

In the neighborhood of the origin we apply the weighted blow-up $(x, y, \nu) = (r\bar{x}, r^2\bar{y}, r\rho)$ where $r \geq 0$ and $(\bar{x}, \bar{y}, \rho) \in \mathbb{S}^2$, to the system (4.2) to which we have added the equation $\nu = 0$. This blows up the origin to a sphere (corresponding to $r = 0$) which is invariant under the flow. Moreover from $\dot{\nu} = 0$ we get that the function $r\rho$ is invariant under the flow. The singular locus $r\rho = 0$ is formed by the plane $\rho = 0$ parametrized by $(\bar{x}, \bar{y}) \in \mathbb{S}^1$ and r ($r = 0$ corresponds to the weighted blow-up of the singularity of (4.2) as $\varepsilon = 0$) together with the sphere $r = 0$, $(\bar{x}, \bar{y}, \rho) \in \mathbb{S}^2$. Because of the geometry the flow has to be studied in charts.

The idea of the method is to study the flow on the singular locus for the different values of the $\bar{\mu}_i$. To study the flow on the sphere $r = 0$ we work in charts. The chart $\rho = 1$ is called the family rescaling while the charts $\bar{x} = \mp 1$ (or $\bar{y} = \pm 1$) allow to study the neighborhood of the circle $r = \rho = 0$ (which corresponds to the usual weighted blow-up of the singularity for $\varepsilon = 0$).

The chart $\rho = 1$ provides phase portraits on the sphere for the different values of $\bar{\mu}_i$. In the charts $x = \mp 1$ we study the neighborhood of the four singular points P_i , $i = 1, \dots, 4$. These are the points at infinity in the chart $\rho = 1$ (infinity being studied in weighted coordinates). Glueing that with the global trajectories outside the neighborhood of the singular point yields limit periodic sets in 3-dimensional space.

In the chart $\rho = 1$ the system has the form

$$\begin{aligned}\dot{\bar{x}} &= \bar{y} + a\bar{x}^2 + \bar{\mu}_2 \\ \dot{\bar{y}} &= \bar{x}\bar{y} + \bar{\mu}_1 + \bar{\mu}_3\bar{y} + O(r).\end{aligned}\tag{4.3}$$

The method consists in identifying all limit periodic sets which we will encounter in the singular set $r\rho = 0$ and in studying the finite cyclicity of each of them. In our case we find the three limit periodic sets appearing in Figure 12 (see also Figure 13 for a 3-dimensional picture). They have to be studied in a three dimensional space, the disk in the middle being the upper half-sphere $r = 0$, $\rho \geq 0$. The use of the invariant foliation $\nu = r\rho = \text{const}$ allows in practice to reduce the study to 2 dimensions.

The points P_1 and P_2 considered previously now become singular points of a 3-dimensional vector field. Looking at them in the respective charts $\bar{x} = \pm 1$, natural coordinates in their neighborhood are given by (r, ρ, \bar{y}_i) . The eigenvalues are given by $\mp a(\varepsilon)$, $\pm a(\varepsilon)$, $\mp(1 - 2a(\varepsilon))$. Hence the normal form depends whether $a(0)$ is rational or irrational. We will treat in detail the simpler case $a(0) \notin \mathbb{Q}$ which contains all the essential ideas. One ingredient is the orbital normal form near P_1 and P_2 . When $a(0) \notin \mathbb{Q}$ the only resonance is between the first two eigenvalues. Because of the invariant foliation the C^k orbital normal form is given by

$$\begin{aligned}\dot{r} &= \mp r \\ \dot{\rho} &= \pm \rho \\ \dot{\hat{y}}_i &= \mp \sigma \hat{y}_i + \hat{y}_i f_\varepsilon^\pm(r\rho)\end{aligned}\tag{4.4}$$

where $\sigma = \frac{1-2a(\varepsilon)}{a(\varepsilon)}$ and $f_\varepsilon^\pm(r\rho) = f_\varepsilon^\pm(\nu) = \sum_{i=1}^k a_i^\pm(\varepsilon)\nu^i$.

Let us come back to the sections $\Sigma_{1,2} = \{x = \mp x_0\}$ defined previously. In the respective charts $\bar{x} = \pm 1$ they correspond to sections with respective equations $r = x_0$, where $r_0 = \rho_0$. Coordinates on the sections

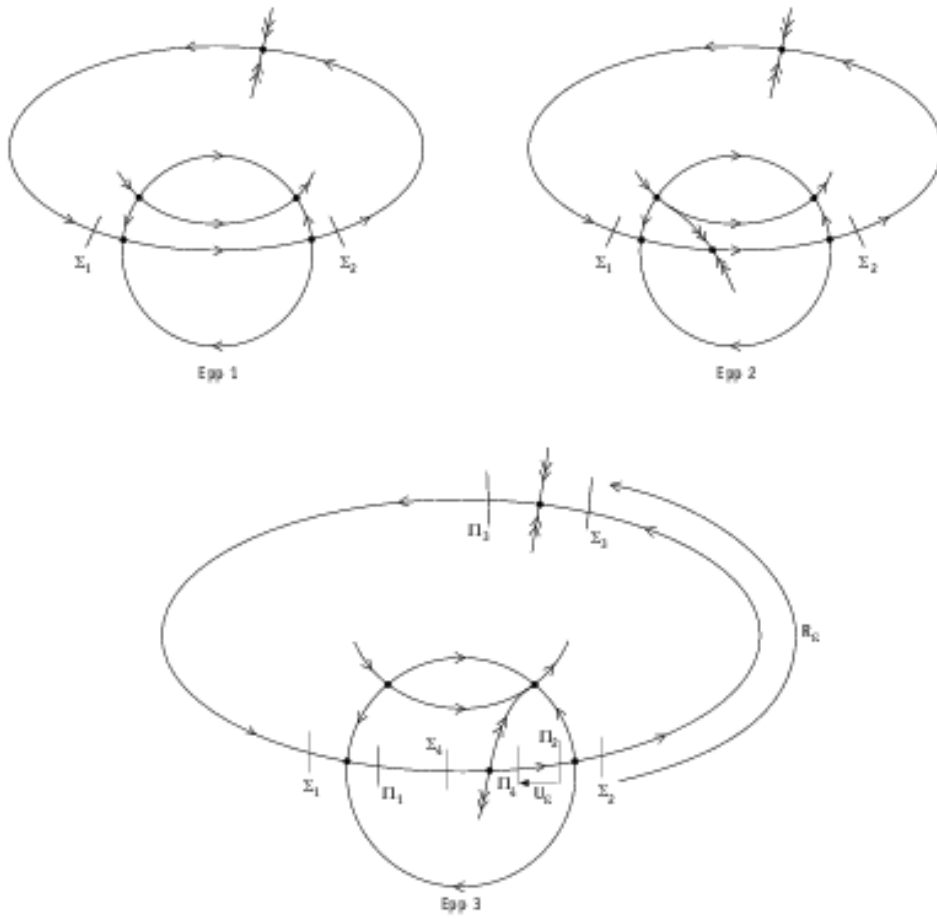


FIGURE 12. The limit periodic sets Epp1, Epp2 and Epp3. The small disk represents the upper half-sphere seen from above

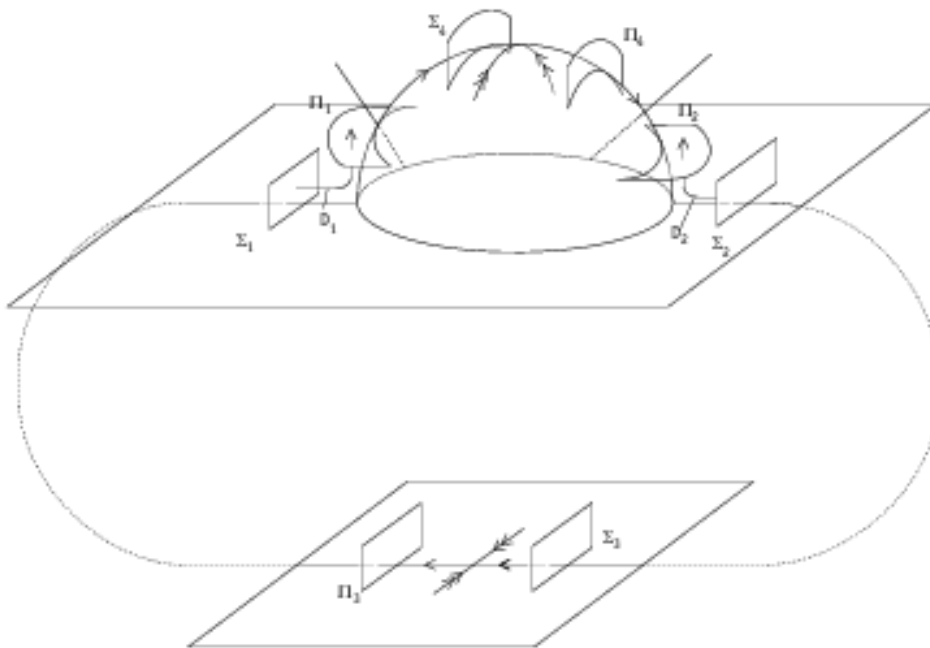


FIGURE 13. The limit periodic set Epp2 and its sections in 3-dimensional space

are ν (related to ρ through $\nu = r_0\rho$) and the variable \hat{y}_i defined in (4.4). Then $\hat{y}_i = \bar{y}_i + o(\bar{y}_i) + O(r) + O(\rho) = \frac{1}{r_0^2}(y_i + o(y_i))$ depends in a C^k way of y_i and the parameters.

Using the blow-up of the family we can now calculate the transition map $T : \Sigma_1 \rightarrow \Sigma_2$. Indeed we decompose it into a composition of three transition maps: two transition maps (Dulac maps) in the neighborhood of P_1 and P_2 and a regular transition map \bar{T} along the blown-up sphere: $T = D_2^{-1} \circ \bar{T} \circ D_1$, where $D_i : \Sigma_i \rightarrow \Pi_i$.

At this point it is important to consider all phase portraits of (4.3). As soon as $\bar{\mu}_1 \neq 0$ there is no passage from P_1 to P_2 on the sphere $r = 0$. Hence the only limit periodic sets listed above correspond to $\bar{\mu}_1 = 0$, i.e. to the existence of an invariant line on which we have either no singular point ($\bar{\mu}_2 > 0$) or a saddle-node ($\bar{\mu}_2 = 0, \bar{\mu}_3 = \pm 1$). The Dulac map corresponding to the passage near P_1 (resp. near P_2 with reverse time) will be the transition map for system (4.4) with $i = 1$ (resp. $i = 2$) from the section $\Sigma_i = \{r = r_0\}$ to a section $\Pi_i = \{\rho = \rho_0\}$, parametrized by $(\nu, \hat{y}_i) = (\rho_0 r, \hat{y}_i)$. The Dulac maps $D_i : \Sigma_i \rightarrow \Pi_i$ are calculated from (4.4) as

$$\begin{aligned} D_i(\nu, \hat{y}_i) &= \left(\nu, \left(\frac{\nu}{\nu_0} \right)^\sigma \hat{y}_i \left(1 + \left(e^{-f_\varepsilon^\pm(\nu) \ln \frac{\nu}{\nu_0}} - 1 \right) \right) \right) \\ &= \left(\nu, \left(\frac{\nu}{\nu_0} \right)^\sigma \hat{y}_i (1 + N_i(\nu, \ln \nu, \varepsilon)) \right) \end{aligned}$$

where $N_i(\nu, \ln \nu, \varepsilon) = -a_1^\pm(\varepsilon)\nu \ln \frac{\nu}{\nu_0} + O(\nu^2(\ln \nu)^2)$ and $\nu_0 = r_0\rho_0$.

The third component in the transition T is the transition map $\bar{T} : \Pi_1 \rightarrow \Pi_2$. The map is regular if $\bar{\mu}_2 > 0$, in which case, because of the invariant foliation, it has the form $(\nu, z) \mapsto (\nu, \bar{T}(\nu, z))$ where $\bar{T}(\nu, z) = A(\nu)z + O(z^2)$ with $A(0) \neq 0$. When $\bar{\mu}_2 = 0$ it is the composition of two regular transition maps and a linear map corresponding to the passage near a saddle-node through central transition. The global form of \bar{T} is the same as in the regular case but the coefficient $A(\nu)$ can be either very small or very large when $\bar{\mu}_2$ varies.

We also have a Dulac map near the saddle-node Q_3 . Near Q_3 the C^k normal form is taken as the product of the usual normal form (depending on ν) with the equation $\dot{\nu} = 0$. Hence the Dulac map has the form $D_3(\nu, u) = (\nu, m_3(\varepsilon)u)$, where $m_3(\varepsilon) \rightarrow 0$ as $\varepsilon \rightarrow 0$.

Finite cyclicity of the limit periodic set Epp1. We consider the return map defined on section Σ_1 in coordinates (ν, \hat{y}_1) . The first coordinate is the map $(\nu, \hat{y}_1) \mapsto \nu$ while the second has a first derivative in \hat{y}_1 smaller than 1. This suffices to prove that Epp1 has cyclicity at most one.

Finite cyclicity of the limit periodic set Epp3. Here there is an additional attracting saddle-node Q_4 on the line $\bar{y} = 0$ on the blown-up sphere. The Dulac map near Q_4 is similar to that of P_3 with a coefficient $m_4(\varepsilon)$ such that $m_4(\varepsilon) \rightarrow 0$ as $\varepsilon \rightarrow 0$. As for Epp1 the cyclicity is at most 1.

Finite cyclicity of the limit periodic set Epp2. In this case we introduce sections Σ_i and Π_i , $i = 3, 4$ near the two saddle-nodes so that the second component of the central transitions are of the form $y_3 \mapsto m_3(\varepsilon)y_3$ and $y_4 \mapsto M_4(\varepsilon)y_4$ where

$$\lim_{\varepsilon \rightarrow 0} m_3(\varepsilon) = 0, \quad \lim_{\varepsilon \rightarrow 0} M_4(\varepsilon) = +\infty.$$

We can choose the normalizing coordinates near Q_3 and Q_4 so that the two transition maps from Π_1 to Σ_4 and from Π_3 to Σ_1 are mere translations. We are left with two C^k -transitions $R_\varepsilon : \Sigma_2 \rightarrow \Sigma_3$ and $U_\varepsilon : \Pi_2 \rightarrow \Pi_4$. We consider the displacement map from Σ_2 to Σ_1 . We only need to consider the second component which can be written as (we denote \hat{y}_2 simply by y):

$$V_\varepsilon(y) = m_3(\varepsilon)R_\varepsilon(y) + \delta_1 - \left(\left(\frac{\nu}{\nu_0} \right)^{-\sigma} (M_4(\varepsilon))^{-1} U_\varepsilon \left(\left(\frac{\nu}{\nu_0} \right)^\sigma y(1 + N_2(\nu)) \right) + \delta_2 \right) (1 + N_1(\nu))^{-1}.$$

The first derivative is given by

$$V'_\varepsilon(y) = m_3(\varepsilon)R'_\varepsilon(y) - M_4(\varepsilon)^{-1}U'_\varepsilon \left(\left(\frac{\nu}{\nu_0} \right)^\sigma y(1 + N_2(\nu)) \right) (1 + N_1(\nu))^{-1}(1 + N_2(\nu)).$$

We consider the equivalent function

$$W_\varepsilon(y) = \frac{R'_\varepsilon(y)}{U'_\varepsilon\left(\left(\frac{\nu}{\nu_0}\right)^\sigma y(1+N_2(\nu))\right)} - (m_3(\varepsilon)M_4(\varepsilon))^{-1}(1+N_1(\nu))^{-1}(1+N_2(\nu)).$$

Then $W_\varepsilon^{(n-1)}(y) \neq 0$ for sufficiently small (y, ε) .

The case $a(0) \in \mathbb{Q}$ is longer to write. However the Dulac maps near P_1 and P_2 have been studied in detail in [RZ1] (in particular the fact that they behave well under derivation). The theorems of [RZ1] ensure that all steps of the proof just done can be reproduced nearly verbatim in the new context. \square

4.2 Application to quadratic vector fields.

Corollary 4.2. *The graphic (I_{10a}^2) (Figure 2) of quadratic systems has finite cyclicity.*

Proof. Originally in [DRR] this graphic was noticed to occur in the family

$$\begin{aligned} \dot{x} &= \lambda x - \mu y + a_{20}x^2 + a_{11}xy + a_{02}y^2 \\ \dot{y} &= \mu x + \lambda y + b_{20}x^2 + b_{11}xy + b_{02}y^2 \end{aligned}$$

with $(\lambda, \mu) \in \mathbb{S}^1$ and $(a_{20}, \dots, b_{02}) \in \mathbb{S}^5$. Using a rotation we can suppose that the hyperbolic singular point at infinity is located along the x -axis, yielding $b_{20} = 0$. By a linear transformation we can assume that the nilpotent singular point is located along the y -axis, yielding $a_{02} = 0$. The point is nilpotent if and only $a_{11} = b_{02} = 0$. Using that the origin is a focus, that the nilpotent point is of elliptic type with the position of the separatrices as in Figure 2 and additional scaling we can finally see that the graphic occurs in a quadratic system of the form:

$$\begin{aligned} \dot{x} &= \delta x - y + Ax^2 \\ \dot{y} &= x + \gamma y + xy \end{aligned}$$

where $A \in (\frac{1}{2}, 1)$.

The additional condition $(\delta - \gamma A)^2 - 4A = 0$ guarantees the existence of a point of multiplicity at least two, so is satisfied when a graphic (I_{10a}^2) occurs but this is not needed in the proof. It is easily checked that the family of graphics through the saddle node ends in a graphic with a hyperbolic saddle with hyperbolicity ratio less than 1. We must show that the map R_0 of Theorem 3.3 is nonaffine on any graphic of the family. As in Theorem 3.2 this will be proved by an analytic extension principle using the fact that the hyperbolicity ratio is different from 1. Indeed R_0 is nonaffine near the limiting graphic which passes through the hyperbolic saddle. We can choose sections in the normalizing coordinates near the saddle-nodes which are analytic. Moreover the point P_2 of the blown-up sphere (Figures 9 and 10) with eigenvalues $(1, -1, \sigma)$ is a node when restricted to the invariant plane $\rho = 0$. Hence the normalizing change of coordinates near P_2 can be taken as the composition of an analytic map: $\bar{y} \mapsto \tilde{y}$, bringing the node to normal form in the plane $\rho = 0$ together with an additional change of coordinates depending on ρ and equal to the identity on the plane $\rho = 0$. The map R_0 is defined between analytic sections parametrized by analytic coordinates. We conclude that the transition map is nonaffine near the limiting graphic, hence nonaffine everywhere. \square

5. ELEMENTARY CATASTROPHIES OF LIMIT CYCLES OCCURRING IN PERTURBATIONS OF THE LIPS

5.1 Bifurcation diagram near a single graphic.

In this section we will concentrate on the simplest situation in which the ‘‘lips’’ occur, namely the configuration represented in Figure 3a, and already considered, with respect to the finite cyclicity problem, in Theorem 3.1. We will continue using some notions introduced in that theorem. Aiming at describing interesting and stable patterns of limit cycles we will impose a number of genericity conditions, to be specified in the text. All our local results – localized near one of the limit periodic sets in the ensemble

– do however also apply to the more complicated situations represented in the Figures 3 and 4. We will deal with local C^∞ ε -families of vector fields with $\varepsilon \in \mathbb{R}^p$.

We locate the semi-hyperbolic point with repelling (resp. attractive) parabolic sector at p_1 (resp. p_2); we should in fact write $p_1(\varepsilon)$ and $p_2(\varepsilon)$ but will not do it for sake of simplicity in notation. For $k > 0$ sufficiently large we use the respective C^k normal forms

$$\begin{cases} \dot{x}_1 = \mu_1(\varepsilon) + \sum_{j=1}^{r-1} b_j(\varepsilon)x_1^j + x_1^{r+1}(1 + a_1(\varepsilon)x_1^r)^{-1} \\ \dot{y}_1 = y_1 \end{cases} \quad (5.1)$$

and

$$\begin{cases} \dot{x}_2 = -\mu_2(\varepsilon) - \sum_{j=1}^{s-1} \bar{b}_j(\varepsilon)x_2^j - x_2^{s+1}(1 + \bar{a}_1(\varepsilon)x_2^s)^{-1} \\ \dot{y}_2 = -y_2 \end{cases} \quad (5.2)$$

with $r, s \geq 1$ and odd. We suppose the chosen graphic to be represented by $y_1 = 0$. In these local coordinates we can now define the “rotational” parameter δ in the regular hh -transition. Let us recall from the proof of Theorem 3.1 that we can reduce the regular hh -transition to an affine map with constant term $\delta(\varepsilon)$.

Like in the proof of Theorem 3.1 we can also consider the regular pp -transition $R(y_1, \varepsilon)$ with respect to the normal form (5.1) and (5.2). Let us introduce

$$a_i(\varepsilon) = \frac{1}{i!} \frac{\partial^i R}{\partial y_1^i}(0, \varepsilon)$$

for $2 \leq i \leq n$, with $k \gg n \geq 2$. As generic conditions we require that

$$a_n(0) \neq 0 \quad (5.3)$$

and that the mapping

$$\varepsilon \mapsto (\delta, \mu_1, \mu_2, b_1, \dots, b_{r-1}, \bar{b}_1, \dots, \bar{b}_{s-1}, a_2, \dots, a_{n-1})(\varepsilon) \quad (5.4)$$

is a submersion at $\varepsilon = 0$.

Theorem 5.1. *Let Γ be a graphic with two semi-hyperbolic points of even multiplicity (Figure 3a), occurring in a C^∞ ε -family of planar vector fields. Suppose that the regular pp -transition (defined on sections parallel to the y -axes in the C^k normalizing coordinates (5.1) and (5.2)) is of order n at $y_1 = 0$, $\varepsilon = 0$ like expressed in (5.3), and that ε is a generic parameter as defined in (5.4). Then, keeping $\mu_1 > 0$ and $\mu_2 > 0$, in any Hausdorff neighborhood W of Γ and in any neighborhood V of $\varepsilon = 0$, the bifurcation diagram of the limit cycles contains a trivial 1-parameter family of elementary catastrophes of codimension $n - 1$.*

Remarks.

- (1) In this theorem we have not described the full bifurcation diagram, and this was on purpose. By Theorem 3.1 we already know the cyclicity to be at most n . In Theorem 5.1 we do not only show the cyclicity to be exactly n , but we also show that all possible stable bifurcations involving at most n limit cycles will occur. We do not intend to study the matching and the interference of these bifurcations of the limit cycles with the bifurcations of the singularities in the unfolding of the semi-hyperbolic points p_1 and p_2 .

Moreover, besides the bifurcations of limit cycles that are “interior” to the chosen y_1 -neighborhood of 0, there are also the bifurcations corresponding to a limit cycle escaping from the chosen neighborhood of the graphic, a problem which we will consider in paragraph 5.2.

- (2) The functions $b_1(\varepsilon), \dots, b_{r-1}(\varepsilon), \bar{b}_1(\varepsilon), \dots, \bar{b}_{s-1}(\varepsilon)$ are not present in condition (5.4) in case the semi-hyperbolic points p_1 and p_2 both are of codimension 1, i.e. $r = s = 1$.
- (3) A complete description of the bifurcations of the polycycle “lips” in generic 3-parameter families was obtained in [KS].

Proof of theorem 5.1. As a consequence of the genericity conditions (5.4) we can, for $\varepsilon \sim 0$, change the parameter $\varepsilon \in \mathbb{R}^p$ to a new parameter

$$\varepsilon = (\varepsilon', \nu)$$

with

$$\varepsilon' = (\delta, \mu_1, \mu_2, b_1, \dots, b_{r-1}, \bar{b}_1, \dots, \bar{b}_{s-1}, a_2, \dots, a_{n-1})$$

and $\nu \in \mathbb{R}^{p-q}$ for $q = r + s + n - 1$. Let us from now on take

$$b_1 = \dots = b_{r-1} = \bar{b}_1 = \dots = \bar{b}_{s-1} = 0, \nu = 0, \quad (5.5)$$

and denote the remaining parameters by

$$\lambda = (\delta, \mu_1, \mu_2, a_2, \dots, a_{n-1}).$$

Let us write y instead of y_1 (the y -coordinate is chosen in a way that $y = 0$ represents the graphic under consideration for $\lambda = 0$).

Like in the proof of Theorem 3.1 we can consider the regular pp -transition $R(y, \varepsilon)$ and the related displacement function $V(y, \varepsilon)$. We can suppose that R is of class C^k , with k finite but as large as we want. Let us restrict to the condition (5.5) and denote $R(y, \varepsilon)$ and $V(y, \varepsilon)$ by respectively $R(y, \lambda)$ and $V(y, \lambda)$.

Under all the conditions that we suppose, we can write

$$V(y, \lambda) = \delta m^{-1}(\lambda) + (\alpha(\lambda) - m^{-1}(\lambda)M^{-1}(\lambda))y + a_2 y^2 + \dots + a_{n-1} y^{n-1} + a_n(\lambda) y^n + \Psi(y, \lambda) \quad (5.6)$$

for some $\alpha(\lambda) > 0$ and with Ψ of class C^k , $\Psi = O(y^{n+1})$, $a_n(0) \neq 0$ and $k \gg n$. Let us recall that

$$m(\lambda) = \exp \left(- \int_{-X}^X \frac{dx_1}{\mu_1 + x_1 h(x_1, \lambda)} \right)$$

and

$$M(\lambda) = \exp \left(\int_{-\bar{X}}^{\bar{X}} \frac{dx_2}{\mu_2 + x_2 \bar{h}(x_2, \lambda)} \right),$$

for some well chosen $X > 0$, $\bar{X} > 0$ and where $h(x_1, \lambda) = x_1^r(1 + a_1(\lambda)x_1^r)^{-1}$, resp. $\bar{h}(x_2, \lambda) = x_2^s(1 + \bar{a}_1(\lambda)x_2^s)^{-1}$.

As such

$$\frac{\partial m}{\partial \mu_1}(\lambda) = \left(\int_{-X}^X \frac{(1 + O(x_1)) dx_1}{(\mu_1 + x_1 h(x_1, \lambda))^2} \right) \cdot m(\lambda), \quad (5.7)$$

which is strictly positive for $\mu_1 > 0$ and X sufficiently small. Similarly we can prove that $M(\lambda) \rightarrow \infty$ for $\mu_2 \rightarrow 0$, and that $\frac{\partial M}{\partial \mu_2}(\lambda) < 0$ for $\mu_2 > 0$ and \bar{X} sufficiently small.

Let us now work along a curve defined by $\delta = 0$, $a_2 = \dots = a_{n-1} = 0$ and $\alpha(\lambda) = m^{-1}(\lambda)M^{-1}(\lambda)$. We consider this curve for $\mu_2 > 0$, where, because of (5.7) and a related property on $\frac{\partial M}{\partial \mu_2}$, we can suppose that it is regular and that it tends to the origin in parameter space for $\mu_2 \rightarrow 0$.

We will now study the bifurcation of limit cycles near $y = 0$ along this curve in parameter space. For that purpose we change expression (5.6) into

$$\bar{V}(y, \lambda, \eta) = \eta_1 + \eta_2 y + a_2 y^2 + \dots + a_{n-1} y^{n-1} + a_n(\lambda) y^n + \Psi(y, \lambda), \quad (5.8)$$

meaning that besides the parameters λ we introduce independent parameters $\eta = (\eta_1, \eta_2)$ that we will also keep close to zero. Expression \bar{V} is C^k in (y, λ, η) and as such we can apply to it the preparation theorem in finite smoothness ([Ba], [L]):

$$\bar{V}(y, \lambda, \eta) = F(y, \lambda, \eta)[y^n + B_{n-1}(\lambda, \eta)y^{n-1} + \dots + B_0(\lambda, \eta)] \quad (5.9)$$

for some $C^{k'}$ functions B_i , $0 \leq i \leq n-1$, vanishing at the origin and F with $F(0,0,0) \neq 0$. In fact if we want here some k' sufficiently larger than n we might need to adapt the previously chosen k . Let us continue denoting k' by k . Along the chosen curve the application

$$(\delta, \mu_1) \mapsto (\eta_1, \eta_2)$$

is a local diffeomorphism near $(0,0)$, for each fixed $\mu_2 > 0$ sufficiently small, and as such the same holds concerning

$$(\delta, \mu_1, a_2, \dots, a_{n-1}) \mapsto (B_0(\lambda, \eta), \dots, B_{n-1}(\lambda, \eta))$$

near $(0, \dots, 0)$.

For each fixed value $\mu_2 > 0$, sufficiently small, we will hence encounter a stable elementary catastrophe of codimension $n-1$ on the zeros of $V(y, \lambda)$. \square

5.2 Bifurcation diagram near an ensemble of graphics.

We continue studying the situation considered in the preceding paragraph 5.1, but instead of merely looking at $y \sim 0$ we will keep $y \in [Y_1, Y_2]$ for some choice $Y_1 < 0 < Y_2$. In this paragraph we aim at fully describing the bifurcation diagram of the limit cycles, as long as these do not interfere with the appearance of singularities. We completely describe it in the particular case $r = s = 1$: it is C^k diffeomorphic to the trivial product of a line segment with the bifurcation set of the zeros of the Complete Tchebychev system $(1, y, \dots, y^n)$ on $[0, 1]$. The same proof provides the description of the bifurcation diagram in the general case where one of r, s is greater than 1 as long as we suppose that the parameter $\varepsilon \in \mathbb{R}^p$ is such that $b_1(\varepsilon), \dots, b_{r-1}(\varepsilon), \bar{b}_1(\varepsilon), \dots, \bar{b}_{s-1}(\varepsilon)$ in (5.1) and (5.2) remain zero. Besides this we want to work as generically as possible. As such we keep condition (5.3), but change (5.4) into the requirement that

$$\varepsilon \mapsto (\delta, \mu_1, \mu_2, a_2, \dots, a_{n-1})(\varepsilon) \tag{5.10}$$

is not only a submersion, but in fact a local diffeomorphism at $\varepsilon = 0$; we hence restrict to $p = n+1$. We can now state the following result:

Theorem 5.2. *Let Γ be a graphic like in Theorem 5.1 occurring in an ε -family with $\varepsilon \in \mathbb{R}^{n+1}$. Suppose that the regular pp-transition is of order n at $y = 0$, for $\varepsilon = 0$, as expressed by (5.3), and let $k \in \mathbb{N}$. Let ε be a generic parameter as defined by (5.10), and let all $b_i(\varepsilon)$ and $\bar{b}_j(\varepsilon)$ in (5.1) and (5.2) be identically zero. If $|Y_1|, |Y_2|$ are sufficiently small then the bifurcation set of the limit cycles given by $y \in [Y_1, Y_2]$, $\mu_1, \mu_2 > 0$ and ε small is C^k diffeomorphic to the trivial product of a line segment with the bifurcation set of the zeros of the Complete Tchebychev System $(1, y, \dots, y^n)$ on $[0, 1]$.*

Proof. We follow the reasoning developed in the proof of Theorem 5.1 and adapt it slightly. Looking at expression (5.9) we can observe that for $(\varepsilon, \eta) \sim 0$ we could introduce $(\mu_1, \mu_2, \delta, B_1, \dots, B_{n-1}, \eta_1, \eta_2)$ as independent parameters instead of (ε, η) . Let us say that it holds for $|\eta_i| \leq E$ with $i = 1, 2$. The bifurcations expressed by (5.9) are then independent of (μ_1, μ_2, δ) . We recall that in fact $\eta_1 = \delta m^{-1}(\lambda)$ and $\eta_2 = \alpha(\lambda) - m^{-1}(\lambda)M^{-1}(\lambda)$. For fixed μ_2 the map $\delta \mapsto \eta_1$ has everywhere a nonzero derivative, while the same is true for $\mu_1 \mapsto \eta_2$, if we fix also (δ, λ) and stay inside the region where (5.9) holds. Indeed, by (5.7) and the boundedness of $\frac{\partial \alpha}{\partial \mu_1}(\varepsilon)$ and η_2 the result easily follows. Outside this region, either $|\eta_1| = |\delta m^{-1}(\lambda)| \geq E$ or $|\eta_2| = |\alpha(\lambda) - m^{-1}(\lambda)M^{-1}(\lambda)| \geq E$. Considering expression (5.8) directly it is clear that, for sufficiently small y , $V(y, \varepsilon)$ will have no zeros for $|\eta_1| \geq |\eta_2|$, while there will be at most one zero for $|\eta_2| \geq |\eta_1|$. In that region the limit cycle has to stay hyperbolic if it exists and since $\frac{\partial \eta_1}{\partial \delta} = m^{-1}(\lambda) > 0$ we see that disappearance of such a limit cycle occurs in the most generic way possible. These observations permit to finish the proof. \square

6.1 General formula.

As we have seen in section 3, in the presence of “lips” the regular pp -transition plays an important role in the study of the cyclicity. We have seen in section 5 that it also plays an essential role in studying the bifurcations of the limit cycles. However it might be quite involved, if not to say technically impossible to control directly – based on the proposed construction – the necessary conditions. Therefore in this paragraph we are going to relate the regular pp -transition R , or more precisely its derivative R' , to some integral, whose essential characteristics are often easier to deal with. Our reduction is based on Poincaré’s formula (see e.g. [ALGM] or [Rc]) for the derivative of a transition map (Poincaré map) near a regular orbit.

Let us consider a C^∞ -family of vector fields X_λ , with $\lambda \in \mathbb{R}^q$, having for each λ a pp -connection between singularities $p_1(\lambda)$ and $p_2(\lambda)$. Like in section 2 and 3 we suppose that – by C^k orbital equivalence (with $k > 0$ sufficiently large) – we can write X_λ near $p_1(\lambda)$ and $p_2(\lambda)$ as the respective normal forms:

$$\begin{cases} \dot{x}_1 = x_1^{r+1}(1 + a_1(\lambda)x_1^r)^{-1} \\ \dot{y}_1 = y_1 \end{cases} \quad (6.1)$$

and

$$\begin{cases} \dot{x}_2 = -x_2^{s+1}(1 + \bar{a}_1(\lambda)x_2^s)^{-1} \\ \dot{y}_2 = -y_2 \end{cases} \quad (6.2)$$

with $r, s \geq 1$ and odd.

Theorem 6.1. *Let X_λ be a C^∞ λ -family of planar vector fields having semi-hyperbolic points $p_1(\lambda)$ and $p_2(\lambda)$ of even multiplicity with respective C^k normal forms (6.1) and (6.2); $k > 0$ is supposed to be sufficiently large. Suppose that there is a pp -connection between $p_1(\lambda)$ and $p_2(\lambda)$ and consider the regular pp -transition map $y_2 = R(y_1, \lambda)$ with respect to the sections $\{x_1 = x'_1\}$ and $\{x_2 = x'_2\}$, for some $x'_1 > 0$ and $x'_2 > 0$; we suppose R to be defined for all $\lambda \in L$ and $y_1 \in [Y_1, Y_2]$; let $Y_1 < y_1^0 < Y_2$ for some y_1^0 . If $\gamma_{y_1}^\lambda$ (resp. $\gamma_{y_1^0}^\lambda$) denotes the X_λ -orbit through the point represented by (x'_1, y_1) (resp. (x'_1, y_1^0)) in (6.1) and R' represents the derivative of R with respect to y_1 , then*

$$R'(y_1, \lambda) = R'(y_1^0, \lambda) \exp \left(\int_{-\infty}^{\infty} (\operatorname{div} X_\lambda(\gamma_{y_1}^\lambda(t)) - \operatorname{div} X_\lambda(\gamma_{y_1^0}^\lambda(t))) dt \right). \quad (6.3)$$

Remarks 6.2.

- (1) The symbol $\int_{-\infty}^{\infty}$ means that we need to integrate over the total orbit $\gamma_{y_1}^\lambda$ (resp. $\gamma_{y_1^0}^\lambda$) in between $p_1(\lambda)$ and $p_2(\lambda)$.
- (2) Because of the presence of $R'(y_1^0, \lambda)$ the formule (6.3) does not really provide an expression for $R'(y_1, \lambda)$ but only for its variation for changing y_1 . However this will not make it less useful. In fact one can always adapt the normalizing coordinates, (cfr. e.g. section 3) in a way that $R'(y_1^0, \lambda) = 1$ at a specifically chosen point y_1^0 .
- (3) The integral expression (6.3) is expressed in terms of the parameter y_1 . In practice however it might be preferable to express R' in some other parameter Y , easier to link to the original coordinate system in which the family X_λ is given. Of course, if we only deal with bifurcations close to a specific 1-parameter family of orbits $\gamma_{y_1^0}^\lambda$, it will be straightforward to pass from the essential properties in the parameter Y to those in y_1 . More specifically, let us take $y_1^0 = 0$ and consider a new parameter $Y = y_1(c(\lambda) + O(y_1))$ with $c(\lambda) \neq 0$. In order to use (6.3) we need to calculate

$$A(y_1, \lambda) = \exp \left(\int_{-\infty}^{\infty} (\operatorname{div} X_\lambda(\gamma_{y_1}^\lambda(t)) - \operatorname{div} X_\lambda(\gamma_0^\lambda(t))) dt \right). \quad (6.4)$$

Suppose that we are able to calculate

$$\bar{A}(Y, \lambda) = \exp \left(\int_{-\infty}^{\infty} (\operatorname{div} X_{\lambda}(\gamma_Y^{\lambda}(t)) - \operatorname{div} X_{\lambda}(\gamma_0^{\lambda}(t))) dt \right),$$

in which we parametrize the set of orbits by the new parameter Y , then we get

$$A(y_1, \lambda) = \bar{A}(Y(y_1), \lambda) = \bar{A}(y_1(c(\lambda) + O(y_1)), \lambda).$$

As such, if $\frac{\partial^{n-1} \bar{A}}{\partial Y^{n-1}}(0, 0) \neq 0$, and $\frac{\partial^i \bar{A}}{\partial Y^i}(0, 0) = 0$ for $i = 1, \dots, n-2$, then the same holds concerning the derivatives $\frac{\partial^j A}{\partial y_1^j}(0, 0)$ for $j = 1, \dots, n-1$.

In view of applying theorem 3.1 this is an important observation. Similar observations can be made if we change A by the derivatives $\frac{\partial A}{\partial \lambda_l}$ for $\lambda = (\lambda_1, \dots, \lambda_q)$ and $l = 1, \dots, q$; taking into account that also $Y(y_1)$ depends on λ .

For a specific application we refer to paragraph 6.2. In that example we will simply write $A(Y, \lambda)$ instead of $\bar{A}(Y, \lambda)$.

Proof of theorem 6.1. Merely for a unified presentation let us apply an extra time reversal to (6.2) in order to change it into:

$$\begin{cases} \dot{x}_2 = x_2^{s+1}(1 + \bar{a}_1(\lambda)x_2^s)^{-1} \\ \dot{y}_2 = y_2, \end{cases}$$

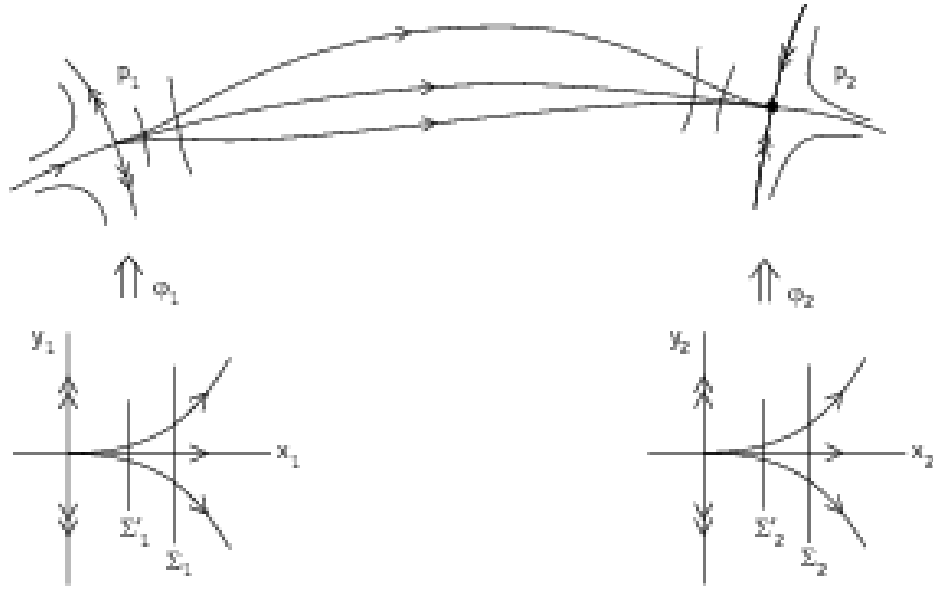


FIGURE 14. Regular pp -transition

In the normal form coordinates we work on the sides $x_1 > 0$ and $x_2 > 0$. Let φ_1 and φ_2 denote the inverses of the transformations bringing the family in normal form (cfr. Figure 14); they are both λ -dependent but we do not express this explicitly. We have chosen sections $\Sigma_1 = \{x_1 = x_1'\}$ and $\Sigma_2 = \{x_2 = x_2'\}$, for some strictly positive x_1' and x_2' , and consider the transition map $R(y_1, \lambda)$ with respect to the y_1 -coordinate on Σ_1 . We restrict to the interval $[Y_1, Y_2]$ of y_1 -values, $Y_1 < Y_2$, without specifying the range of image values and we also consider y_1^0 with $Y_1 < y_1^0 < Y_2$; we keep $\lambda \in L$.

From Poincaré's formula [Rc] we get

$$R'(y_1, \lambda) = \frac{A_1(y_1)}{A_2(y_1)} \exp \left(\int_{T_{x_1' x_2'}} \operatorname{div} X(\gamma_{y_1}(t)) dt \right) \quad (6.5)$$

with

$$A_1(y_1) = (\det D\varphi_1(x'_1, y_1))((x'_1)^{r+1}(1 + a_1(\lambda)(x'_1)^r)^{-1}) \quad (6.6)$$

$$A_2(y_1) = (\det D\varphi_2(x'_2, y_2(y_1)))(x'_2)^{s+1}(1 + \bar{a}_1(\lambda)(x'_2)^s)^{-1}, \quad (6.7)$$

$y_2(y_1) = R(y_1, \lambda)$, $\gamma_{y_1}(t)$ is the X_λ -orbit related to (x'_1, y_1) and $T_{x'_1, x'_2}$ denotes the time to travel along the orbit γ_{y_1} from $\varphi_1(\Sigma_1)$ to $\varphi_2(\Sigma_2)$; let us also remark that in the expressions (6.5), (6.6), (6.7), and for the sake of simplicity in notation, we have not explicitly expressed the λ -dependence of a number of functions.

Let us now also consider a second pair of sections $\Sigma'_1 = \{x_1 = x''_1\}$ and $\Sigma'_2 = \{x_2 = x''_2\}$ with $0 < x''_1 < x'_1$ and $0 < x''_2 < x'_2$. In the normal form coordinates the passage from Σ_1 to Σ'_1 (resp. Σ_2 to Σ'_2) has the expression $y_1 \rightarrow m_{x'_1, x''_1} y_2$ (resp. $y_2 \rightarrow M_{x'_2, x''_2} y_2$). We also get:

$$R'(y_1, \lambda) = \frac{m_{x'_1, x''_1} A'_1(y_1)}{M_{x'_2, x''_2} A'_2(y_1)} \exp \left(\int_{T_{x''_1, x''_2}} \operatorname{div} X(\gamma_{y_1}(t)) dt \right), \quad (6.8)$$

with

$$A'_1(y_1) = (\det D\varphi_1(x''_1, m_{x'_1, x''_1} y_1))((x''_1)^{r+1}(1 + a_1(\lambda)(x''_1)^r)^{-1}$$

$$A'_2(y_1) = (\det D\varphi_2(x''_2, M_{x'_2, x''_2} y_2(y_1)))(x''_2)^{s+1}(1 + \bar{a}_1(\lambda)(x''_2)^s)^{-1}$$

and $T_{x''_1, x''_2}$ denotes the time to travel along the orbit γ_{y_1} from $\varphi_1(\Sigma'_1)$ to $\varphi_2(\Sigma'_2)$.

Let us now look to what happens when we fix x'_1 and x'_2 but let x''_1 and x''_2 tend to zero. Using the fact that

$$\lim_{(x''_1, x''_2) \rightarrow (0,0)} \frac{A'_1(y_1)}{A'_2(y_1)} \cdot \frac{A'_2(y_1^0)}{A'_1(y_1^0)} = 1$$

we can obtain from (6.8) the required integral expression (6.3), in which we have written X_λ , $\gamma_{y_1}^\lambda$ and $\gamma_{y_1^0}^\lambda$ in order to stress the dependence on λ , and where the symbol $\int_{-\infty}^{\infty}$ means that we need to integrate over the total orbit γ_{y_1} in between $p_1(\lambda)$ and $p_2(\lambda)$. \square

Remark on analytic families. In working with analytic families we can apply the results of section 2, namely the fact that in using C^k normalizing coordinates we can use “analytic sections” in order to define the regular transition map near the pp -connection. Also the dependence on λ remains analytic as long as the “formal invariants” are kept constant. As such if the formal invariants remain unchanged, then the application $R(y_1, \lambda)$ as well as the expression $A(y_1, \lambda)$ in (6.4) will be analytic.

This could be interesting in view of proceeding similarly to what has been done in the study of analytic unfoldings of a Hamiltonian regular cycle (homoclinic loop see e.g. [R2]); a decomposition of $R(y_1, \lambda) - R'(0, \lambda)y_1$ in its ideal of coefficients at $\lambda = 0$, might permit to obtain a finite cyclicity result under some mild conditions. We will not work this out.

6.2 Application to a specific example.

In order to get the flavour of how the preceding paragraphs can be applied we will consider a specific example

Proposition 6.3.

(1) Any graphic of “lip” type in the following system

$$\begin{aligned} \dot{y} &= y \cos \theta + y^n \\ \dot{\theta} &= \sin^2 \theta \end{aligned} \tag{6.9}$$

on the cylinder $(\theta, y) \in S_1 \times \mathbb{R}$ has finite cyclicity inside any C^∞ family of vector fields. The graphic $y = 0$ has cyclicity $\leq n$.

(2) Inside the particular family

$$\begin{cases} \dot{y} = y \cos \theta + y^2 Q(y, \lambda) + \rho \\ \dot{\theta} = 4(\sin^2 \frac{\theta}{2} + \varepsilon_1)(\cos^2 \frac{\theta}{2} + \varepsilon_2) \end{cases} \tag{6.10}$$

with

$$Q(y, \lambda) = \sum_{i=1}^{n-2} \lambda_i y^{i-1} + y^{n-2}$$

and $\lambda = (\lambda_1, \dots, \lambda_{n-2}) \in \mathbb{R}^{n-2}$ the cyclicity of the graphic $y = 0$ is exactly n and the bifurcation diagram contains a trivial 1-parameter family of elementary catastrophes of codimension $n - 1$ as in Theorem 5.1.

Proof. Let us discuss briefly the proof of (1), parts of which will be done in the proof of (2). Indeed, in the proof of (2) we will need to calculate the regular pp -transition map $R(y_1, \varepsilon_1, \varepsilon_2, \rho, \lambda_1, \dots, \lambda_{n-2})$. Let us call $R_0(y_1) = R(y_1, 0, 0, 0, 0, \dots, 0)$. The calculation will yield in particular $R_0^{(n)}(0) \neq 0$. Hence the cyclicity of the graphic $y = 0$ is $\leq n$ in any C^∞ perturbation of (6.9) by Theorem 3.1.

Moreover as discussed in Section 2 and since (6.9) is analytic it is possible to define $R_0 : \Sigma \rightarrow \Pi$ on analytic sections parametrized by analytic coordinates. Hence for any y_1^* in Σ there exists $n(y_1^*) \in \mathbb{N}$ such that $R_0^{n(y_1^*)}(y_1^*) \neq 0$, yielding that the graphic of “lip” type through y_1^* has cyclicity $\leq n(y_1^*)$. This finishes the proof of (1) modulo $R_0^{(n)}(0) \neq 0$.

For the proof of (2) we will only study (6.10) for $y \sim 0$, and $(\varepsilon_1, \varepsilon_2, \rho, \lambda_1, \dots, \lambda_{n-2}) \sim (0, \dots, 0)$.

If we put $\rho = \varepsilon_1 = \varepsilon_2 = 0$ we have the λ -family

$$X_\lambda : \begin{cases} \dot{y} = y \cos \theta + y^2 Q(y, \lambda) \\ \dot{\theta} = \sin^2 \theta. \end{cases} \tag{6.11}$$

The unique singularities of X_λ , for y small, are at $p_1 = (0, 0)$ and $p_2 = (\pi, 0)$. Both are saddle-nodes of codimension 1; their “formal invariants” are both zero, and hence independent of ε so that, in accordance with the last remark in section 6.1, we expect an analytic regular pp -transition, both in y and λ , if we choose an analytic parameter analytically depending on λ . The local phase portrait near $\{y = 0\}$ is represented in Figure 15.

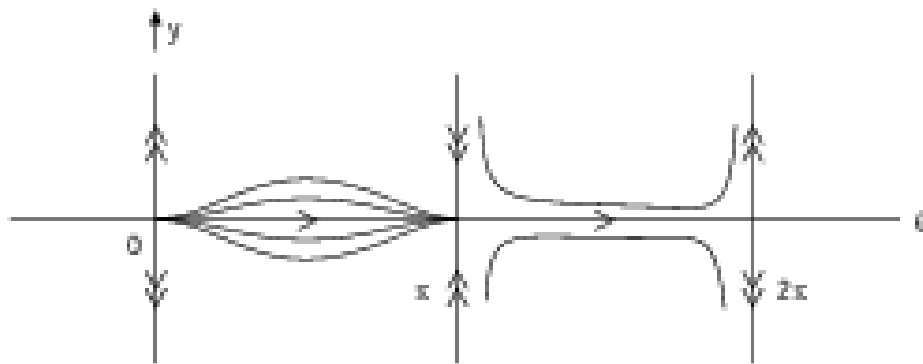


FIGURE 15. Phase portrait of (6.11)

To give interesting information on the bifurcation diagram of the limit cycles of (6.10) near $\{y = 0\}$ and $(\varepsilon_1, \varepsilon_2, \delta, \lambda)$ small, we can try to apply Theorem 5.1. Since both semi-hyperbolic points have codimension 1 there will be no need to check the genericity conditions on the b_i and \bar{b}_j in (5.4).

It is easy to check that the presence of $(\varepsilon_1, \varepsilon_2, \rho)$ permits to show the genericity conditions on (δ, μ_1, μ_2) in (5.4). The necessary properties near p_1 and p_2 follow from standard normal form calculations; in fact $(\mu_1, \mu_2) = (0, 0)$ iff $(\varepsilon_1, \varepsilon_2) = (0, 0)$. In considering the regular hh -transition with respect to the C^k normal forms near p_1 and p_2 , it will not be difficult to show that $\frac{\partial \delta}{\partial \rho} \neq 0$ in the region under consideration. There hence remains to study the regular pp -transition $R(y_1, \varepsilon_1, \varepsilon_2, \rho, \lambda_1, \dots, \lambda_{n-2})$, where we can restrict to $(\varepsilon_1, \varepsilon_2, \rho) = (0, 0, 0)$; let us denote the restriction by $R(y_1, \lambda)$. On $R(y_1, \lambda)$ we can apply the integral expression (6.3), introduced in theorem 6.1. In fact, as announced in the third part of Remarks 6.2, we will not directly calculate $A(y_1, \lambda)$, as defined in (6.4), but change y_1 by a new parameter Y . As new parameter describing the orbits in the lips we use the y -coordinate Y at which the orbit cuts $\{\theta = \frac{\pi}{2}\}$. As reference orbit (choice of $\gamma_{y_1^0}$) in the formula (6.4) we choose $\{Y = 0\}$, inducing

$$A(Y, \lambda) = \exp \left(\sum_{i=1}^{n-2} (i+1) \lambda_i I_i(Y, \lambda) + n I_{n-1}(Y, \lambda) \right)$$

with

$$I_k(Y, \lambda) = \int_0^\pi \frac{(y(Y, \theta, \lambda))^k}{\sin^2 \theta} d\theta$$

and where $\theta \in]0, \pi[\rightarrow y(Y, \theta, \lambda)$ describes the orbit with $y(Y, \frac{\pi}{2}, \lambda) = Y$.

If we write

$$C_k = \int_0^\pi \frac{(\frac{\partial y}{\partial Y}(0, \theta, 0))^k}{\sin^2 \theta} d\theta > 0$$

then clearly $\frac{\partial^j I_k}{\partial Y^j}(0, \lambda) = 0$ for $j < k$ and $\frac{\partial^k I_k}{\partial Y^k}(0, \lambda) = (k!)C_k + O(\lambda)$, inducing that

$$I_k(Y, \lambda) = (C_k + O(\lambda))Y^k + O(Y^{k+1}).$$

As such

$$A(Y, \lambda) = 1 + \sum_{i=1}^{n-2} (i+1) F_i(\lambda) Y^i + n(C_{n-1} + O(\lambda))Y^{n-1} + O(Y^n)$$

with $F_1(\lambda) = C_1 \lambda_1 + O(|\lambda|^2)$ and $F_i(\lambda) = C_i \lambda_i + O(\lambda_1, \dots, \lambda_{i-1}) + O(|\lambda|^2)$, for $2 \leq i \leq n-2$; $(\lambda_1, \dots, \lambda_{n-2}) \mapsto (F_1(\lambda), \dots, F_{n-2}(\lambda))$ is a local diffeomorphism at $\lambda = 0$.

Knowing that $Y = c(\lambda)y_1 + O(y_1^2)$ for some $c(\lambda) > 0$, we get :

$$\begin{aligned} A(y_1, \lambda) &= 1 + \sum_{i=1}^{n-2} (i+1) [(c(\lambda))^i C_i \lambda_i + O(\lambda_1, \dots, \lambda_{i-1}) + O(|\lambda|^2)] y_1^i \\ &\quad + n((c(\lambda))^{n-1} C_{n-1} + O(\lambda)) y_1^{n-1} + O(y_1^n). \end{aligned} \tag{6.12}$$

If we take y_1 in a way that $R'(0, \lambda) = 1$ – choice which is always permitted – then in expression (6.12) we can write $R'(y_1, \lambda)$ instead of $A(y_1, \lambda)$; let us write it as

$$R'(y_1, \lambda) = 1 + \sum_{i=1}^{n-2} (i+1) G_i(\lambda) y_1^i + n G_{n-1}(\lambda) y_1^{n-1} + O(y_1^n) \tag{6.13}$$

for the appropriate choice of $G_i(\lambda)$, $i = 1, \dots, n-1$. In particular $G_{n-1}(\lambda) \neq 0$.

By integrating (6.13) we get:

$$R(y_1, \lambda) - R(0, \lambda) = y_1 + \sum_{i=1}^{n-2} G_i(\lambda)y_1^{i+1} + G_{n-1}(\lambda)y_1^n + O(y_1^{n+1}),$$

which, for $y_1 \sim 0$ and $\lambda \sim 0$, clearly satisfies the requirements needed in Theorem 5.1. This also implies $R_0^{(n)}(0) \neq 0$ as required in the proof of (1). It guarantees that the bifurcation diagram of the limit cycles of small amplitude ($y_1 \sim 0$) of (6.10), for $(\varepsilon_1, \varepsilon_2, \rho, \lambda) \sim (0, 0, 0, 0)$ and with $\varepsilon_1 > 0$ and $\varepsilon_2 > 0$, contains a trivial 1-parameter family of elementary catastrophes of codimension $n - 1$.

In combination with theorem 3.1 we also find that the local cyclicity of the graphic inside the family (6.10) is exactly n . \square

ACKNOWLEDGEMENTS

The authors are grateful to Robert Roussarie and Sergey Yakovenko for helpful discussions.

REFERENCES

- [ALGM] A. Andronov, E. Leontovich, I Gordon and A. Maier, *Theory of bifurcations of dynamical systems on the plane*, Israel Program Sci. Trans. (1971).
- [Ba] G. Barbançon, *Théorème de Newton pour les fonctions de classe C^r* , Ann. Sci. École Norm. Sup. **5** (1972), 435–457.
- [B] P. Bonckaert, *Conjugacy of vector fields respecting additional properties*, J. Dynamical and Control Systems **3** (1997), 419–432.
- [DGR] F. Dumortier, A. Guzmán and C. Rousseau, *Finite cyclicity of elementary graphics surrounding a focus or center in quadratic systems*, in preparation (2000).
- [DRR] F. Dumortier, R. Roussarie and C. Rousseau, *Hilbert’s 16th problem for quadratic vector fields*, J. Differential Equations **110** (1994), 86–133.
- [DRS] F. Dumortier, R. Roussarie and J. Sotomayor, *Bifurcations of cuspidal loops*, Nonlinearity **10** (1997), 1369–1408.
- [EM] M. El Morsalani, *Perturbations of graphics with semi-hyperbolic singularities*, Bull. Sciences Mathématiques **120** (1996), 337–366.
- [GR] A. Guzmán and C. Rousseau, *Genericity conditions for finite cyclicity of elementary graphics*, J. Differential Equations **155** (1999), 44–72.
- [HKM] H. Hukuhara, T. Kimura and T. Matuda, *Équations différentielles ordinaires du premier ordre dans le champ complexe*, Math. Soc. of Japan, 1961.
- [I1] Yu. Ilyashenko, *Dulac’s memoir “On limit cycles” and related topics of the theory of differential equations*, Uspekhi Matematicheskikh Nauk, **40 n 6** (1985), 41–70.
- [I2] Yu Ilyashenko, *Nonlinear Stokes phenomena*, Advances in Soviet Mathematics, volume 14, American Mathematical Society, 1993, 1-55.
- [IL] Yu Ilyashenko and W.Li, *Nonlocal Bifurcations*, Mathematical Surveys and Monographs, vol. 66, AMS Providence, Rhode Island, 1999.
- [IY1] Yu Ilyashenko and S. Yakovenko, *Finitely-smooth normal forms of local families of diffeomorphisms and vector fields*, Russian Math. Surveys **46** (1991), 1–43.
- [IY2] Yu Ilyashenko and S. Yakovenko, *Finite cyclicity of elementary polycycles*, American Mathematical Society Translations, series 2 **165** (1995), 21–95.
- [KS] A Kotova and V Stanzo, *On few-parameter generic families of vector fields on the two-dimensional sphere*, American Mathematical Society Translations, series 2 **165** (1995), 155–201.
- [L] M. G. Lasalle, *Une démonstration du théorème de division pour les fonctions différentiables*, Topology **12** (1973), 41–62.
- [MR] J. Martinet and J.-P. Ramis, *Problèmes de modules pour des équations différentielles non linéaires du premier ordre*, Publ. Math., Inst. Hautes Étud. Sci. **55** (1982), 63–164.
- [Rc] C. Robinson, *Dynamical Systems, Stability, Symbolic Dynamics and Chaos*, CRC Press (1995).
- [R1] R. Roussarie, *A note on finite cyclicity and Hilbert’s 16th problem*, Springer Lecture Notes in Mathematics **1331** (1988), 161–168.
- [R2] R. Roussarie, *Cyclicité finie des lacets et des points cuspidaux*, Nonlinearity **2** (1989), 73–117.
- [RZ1] H. Zhu and C. Rousseau, *Finite cyclicity of graphics through a nilpotent singularity of elliptic or saddle type*, to appear in J. Differential Equations.
- [RZ2] H. Zhu and C. Rousseau, *Graphics with a nilpotent singularity in quadratic systems and Hilbert’s 16th problem*, in preparation (2000).